A CONTINUUM MODEL FOR DECOHERENCE IN 1D TRANSPORT

A THESIS SUBMITTED TO
THE GRADUATE SCHOOL OF NATURAL AND APPLIED SCIENCES
OF
MIDDLE EAST TECHNICAL UNIVERSITY

BY

SELMA ŞENOZAN

IN PARTIAL FULFILLMENT OF THE REQUIREMENTS

FOR

THE DEGREE OF MASTER OF SCIENCE

IN

PHYSICS

AUGUST 2005

Approval of the Graduate School of Natural and Applied Sciences.

Prof. Dr. Canan Özgen
Director

I certify that this thesis satisfies all the requirements as a thesis for the degree of Master of Science.

Prof. Dr. Sinan Bilikmen
Head of Department

This is to certify that we have read this thesis and that in our opinion it is fully adequate, in scope and quality, as a thesis for the degree of Master of Science.

Assist. Prof. Dr. Sadi Turgut
Supervisor

Examining Committee Members

Prof. Dr. Mehmet Tomak (METU, PHYS) _____

Assist. Prof. Dr. Sadi Turgut (METU, PHYS) _____

Assist. Prof. Dr. Oguz Gülseren (BILKENT,PHYS) _____

Assoc. Prof. Dr. Ali Murat Güler (METU, PHYS) _____

Assoc. Prof. Dr. Enver Bulur (METU, PHYS) _____

"I hereby declare that all information in this document has been obtained and presented in accordance with academic rules and ethical conduct. I also declare that, as required by these rules and conduct, I have fully cited and referenced all material and results that are not original to this work."

Name Surname : Selma Şenozan

Signature :

ABSTRACT

A CONTINUUM MODEL FOR DECOHERENCE IN 1D TRANSPORT

Şenozan, Selma

M.S., Department of Physics

Supervisor: Assist. Prof. Dr. Sadi Turgut

AUGUST 2005, 48 pages

In this thesis we study the conductance of a one dimensional conductor in the presence of dephasing. Dephasing effects are modelled after generalizing Büttiker's dephasing model (Phys. Rev. B 33, 3020 (1986)) to a continuous one. Infinitely many electron reservoirs are coupled to the conductor as phase breakers and the method for calculating the conductance is presented. We investigate how this continuum decoherence effect the conductance of a wire, with single and double rectangular barriers.

Keywords: Decoherence,Landauer-Büttiker Formalism, continuous decoherence model

ÖZ

BİR BOYUTTA TRANSPORT İÇİN SÜREKLİ BİR UYUM KAYBI MODELİ

Şenozan, Selma
Yüksek Lisans, Fizik Bölümü
Tez Yöneticisi: Assist. Prof. Dr. Sadi Turgut

AĞUSTOS 2005, 48 sayfa

Bu yüksek lisans tezinde bir boyutta bir iletkenin uyum kaybı göz önüne alınarak iletkenliği çalışılmıştır. Büttiker'in uyum kaybı modeli (Phys. Rev. B 33, 3020 (1986)) genelleştirilerek uyum kaybı üzerine sürekli bir model oluşturulmuştur. Faz değiştirici olarak iletkenin üzerine sonsuz sayıda elektron rezervuarları bağlanmış ve iletkenliğin hesaplanması için bir metod geliştirilmiştir. Bu sürekli uyum kaybının bir boyutta bir telin iletkenliğini nasıl etkilediği tel üzerine tek ve ikili potansiyel bariyerler yerleştirilerek incelenmiştir.

Anahtar Kelimeler: Uyum kaybı, Landauer-Büttiker Formülasyonu, sürekli decoherence modeli

To my Büdü

ACKNOWLEDGMENTS

I would like to thank to Dr. Sadi Turgut for his support and supervision in this work. I would also like to thank to my friend Emre Taşcı for helping me on Xfig and Alper Teke for helping me on LATEX and Deniz for saving me many hours by washing the dishes. And lots of thanks to Büdü for encouraging, supporting, assisting, reinforcing and for loving me. And many many thanks to my family.

TABLE OF CONTENTS

LIST OF FIGURES

FIGURES

CHAPTER 1

INTRODUCTION

Research in conductance properties has grown tremendously in the past two decades. Advances in fabrication and material growth technologies have enabled researches to fabricate devices whose dimensions are intermediate between the macroscopic and the microscopic length scales, and hence called mesoscopic. What makes important these mesoscopic structures is that at these scales an electron no longer behaves simply as a classical particle, but begins to exhibit quantum mechanical effects. Consequently, there exists an enormous interest in the investigation of quantum transport in mesoscopic systems.

Most of the recent work on mesoscopic conductors has largely been based on GaAs-AlGaAs heterojunctions where a thin two-dimensional conducting layer is formed at the interface between GaAs and AlGaAs. Because of two important properties these semiconductor materials are very special for forming two-dimensional electron gas (2DEG). First, 2DEG in a GaAs-AlGaAs heterojunction has Fermi wavelength which is about a hundred times larger than in a metal and second, in these heterolayers electrons have extremely low scattering rates and high mobility at low temperatures. Because of these properties it is possible to study a constriction with an opening, which is comparable to the Fermi wavelength and much smaller than the mean free path. Such constrictions are called quantum point, or ballistic contact. If the width of the opening of the constriction can be varied, one can adjust the position of the one-dimensional electron-energy subbands (modes,channels) with respect to Fermi level. Such a quantum point contact of adjustable width can usually

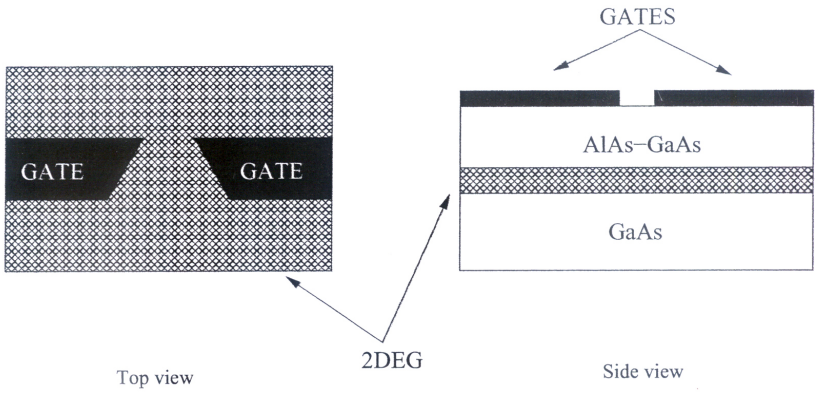

Figure 1.1: Schematic view of the metal gate used to define a constriction to observe conductance quantization.

be achieved by using split-gate technique developed by Thornton T. J. [1] A typical geometry is shown in Fig. 1.1. On top of the heterostructure two metal gates are deposited and by the application of a negative voltage to the gate, which depletes the electrons of the 2DEG beneath it, a narrow channel called point contact is defined. Low-temperature conductance versus gate voltage data in split-gate structures exhibits conductance steps quantized in integer multiples of conductance quantum $G_0 = 2e/h^2$, which is reported by van Wees [2] and Wharam [3] independently in 1988. This phenomenon is usually treated with the Landauer-Büttiker formalism [4] which explains it in a very simple way.

Interference of electron waves (both constructive and destructive) play an important role in shaping the transport properties of mesoscopic structures. However, a process called dephasing, which is very effective in macroscopic length scales, has important effects in mesoscopic scales as it prevents quantum mechanical wave interference. [5, 6] It arises from the interaction of electrons with other excitations in the environment, phonons and other electrons. Consider for example the two-slit experiment. If we do not try to find out which slit the particle passes through, the two waves from both slits interfere at the screen, either constructively or destructively depending on the position on the screen. We can try to determine which slit the particle passes through, by placing an atom in front of one of the slits. [7] The collision of the particle with the atom change the momentum of the particle drastically in the

course of scattering. The deflection of the electron is random since the momentum transferred to the electron is random. In this case, the wave that comes from the atom after hitting it and the wave that comes from the other slit loses coherence and the interference on the screen disappears. In general, if a particle have some changes in the course of interaction with the environment it loses its phase and interference pattern vanishes. This is called dephasing or decoherence. [7, 8, 9, 10]

1.1 Scattering Matrix in 1D

Scattering of waves when they are passing through a region with varying potential can be described by a single 2×2 matrix called the scattering matrix. Consider a potential barrier like in Fig. 1.2 which acts like a scatterer. Here we consider only the case where $V(x) = 0$ on the left and right sides of the scatterer. The Schrödinger's equation for this system is

$$\frac{-\hbar^2}{2m}\frac{d^2\psi(x)}{dx^2} + V(x)\psi(x) = E\psi(x) \quad . \tag{1.1}$$

For the left incident wave with amplitude 1, as in Fig. 1.3, the wavefunction on the left-hand and right-hand sides of the sactterer can be written as

$$\psi_L(x) \quad = \quad \begin{cases} \left(e^{ikx} + re^{-ikx}\right) & \text{,left} \\ \left(te^{ikx}\right) & \text{,right} \end{cases}$$

where t is called the transmission amplitude and r is called the reflection amplitude for the left incident waves.

Same can be done for the right incident wave,as in Fig. 1.4. So the wavefunction on the left and right-hand sides of the scatterer can be written as

$$\psi_R(x) \quad = \quad \begin{cases} \left(t'e^{-ikx}\right) & \text{,left} \\ \left(e^{-ikx} + r'e^{ikx}\right) & \text{,right} \end{cases}$$

Here t' and r' are called as transmission and reflection amplitudes, respectively for the right incident waves.

Any arbitrary solution of the wave equation (1.1) can be expressed as a superposition of these two particular solutions as

$$\psi(x) = A\psi_L + B\psi_R \quad .$$

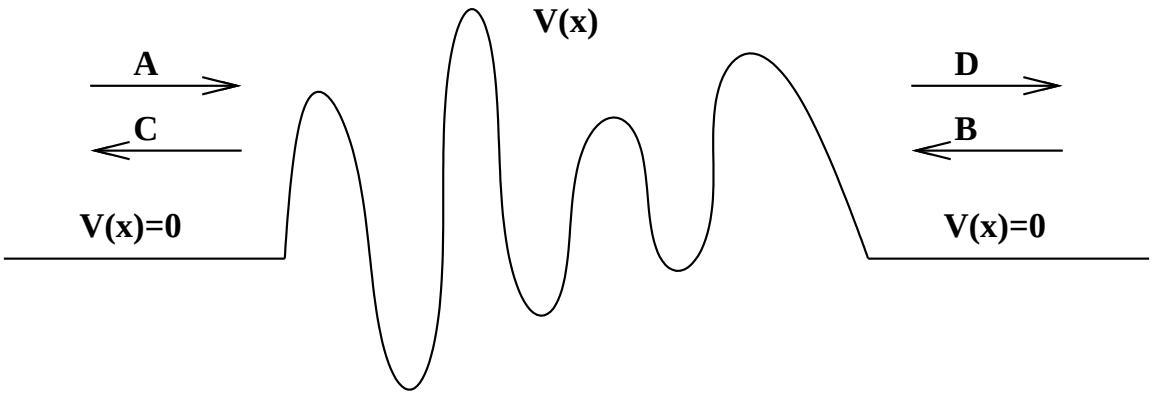

Figure 1.2: Scattering problem for some potential barrier. Incoming and outgoing wave amplitudes are shown.

$$\psi(x) \quad = \quad \begin{cases} \left(Ae^{ikx} + Ce^{-ikx}\right) & \text{,left} \\ \left(De^{ikx} + Be^{-ikx}\right) & \text{,right} \end{cases} \tag{1.2}$$

Here A and B are called incoming wave amplitudes and C and D are called outgoing wave amplitudes.

Outgoing wave amplitudes C and D can be determined in terms of the incoming wave amplitudes A and B as

$$C = rA + t'B \quad , \tag{1.3}$$

$$D = tA + r'B \quad . \tag{1.4}$$

The scattering matrix, S, is defined as the coefficient matrix in the relations between outgoing and incoming amplitudes.

$$S = \begin{pmatrix} r & t' \\ t & r' \end{pmatrix}$$

$$\begin{pmatrix} C \\ D \end{pmatrix} = \begin{pmatrix} r & t' \\ t & r' \end{pmatrix} \begin{pmatrix} A \\ B \end{pmatrix}$$

The scattering matrix S has to be unitary, i.e., $SS^{\dagger} = \mathbf{1}$, due to current conservation. [4] Current conservation can be expressed as

$$\overrightarrow{\nabla}.\overrightarrow{J} = 0 \quad . \tag{1.5}$$

where

$$\overrightarrow{J} = \frac{\hbar}{2mi}(\psi^*.\overrightarrow{\nabla}\psi - \overrightarrow{\nabla}\psi^*.\psi) \quad ,$$

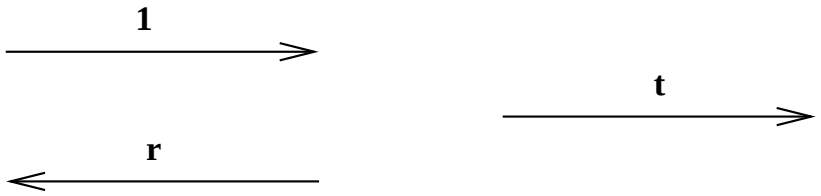

Figure 1.3: For the left incoming wave with amplitude 1 and reflection and transmission amplitude, r and t, respectively.

Figure 1.4: For the right incoming wave with amplitude 1 and reflection and transmission amplitude, r' and t', respectively.

which is valid for any wave function with fixed energy.

In 1D, the relation in Eq. (1.5) can be expressed as

$$\frac{dJ_x}{dx} = 0 \quad ,$$

which implies that J_x is constant. Applying this to the general wave function in Eq. (1.2) we get

$$\mid A \mid^2 + \mid B \mid^2 = \mid D \mid^2 + \mid C \mid^2 \quad , \tag{1.6}$$

which can be interpreted as sum of incoming probabilities being equal to sum of outgoing probabilities. This relation implies the unitarity of S matrix

$$SS^\dagger = S^\dagger S = \mathbf{1} \quad .$$

These can be summarized as the following three relations

$$\begin{aligned} \mid r \mid^2 + \mid t \mid^2 &= 1 \quad , \\ \mid r' \mid^2 + \mid t' \mid^2 &= 1 \quad , \\ rt'^* + tr'^* &= 0 \quad . \end{aligned}$$

The first one is a special case of Eq. (1.6) when ψ_L is used. In that case, $T = \mid t' \mid^2$ can be interpreted as transmission probability. Similarly, the second one is a special case

of Eq. (1.6) when ψ_R is used. The transmission probability for the incoming waves from the right-hand side is denoted by prime.

Time reversal symmetry implies that if $\psi(x)$ is a solution of the wave equation (1.1) then its complex conjugate, $\psi(x)^*$, is also a solution. In that case

$$\psi(x) \quad = \quad \begin{cases} \left(C^* e^{ikx} + A^* e^{-ikx}\right) & \text{,left} \\ \left(B^* e^{ikx} + D^* e^{-ikx}\right) & \text{,right} \end{cases}$$

is a wave where incoming wave amplitudes are C^* and D^* and the outgoing amplitudes are A^* and B^*. These amplitudes also must be related by the S-matrix as

$$\begin{pmatrix} A^* \\ B^* \end{pmatrix} = S \begin{pmatrix} C^* \\ D^* \end{pmatrix}$$

By taking the complex conjugate we get

$$\begin{pmatrix} A \\ B \end{pmatrix} = S^* \begin{pmatrix} C \\ D \end{pmatrix} = S^* S \begin{pmatrix} A \\ B \end{pmatrix}$$

which implies that $S^* S = \mathbf{1}$ and therefore $S^* = S^\dagger$. This implies that S is a symmetric matrix, i.e. $S = S^T$. [4] In our case, this gives one more relation $t = t'$.

1.2 Landauer Single Channel Formulation

Landauer has obtained a very useful relationship (called Landauer relation) between the conductance of a one dimensional wire and the scattering matrix of the wire. [11, 12] Later on Büttiker generalized this relationship into a what is called as Landauer-Büttiker formalism. [4, 13]

Consider a general barrier problem in a one dimensional conductor, shown in Fig. 1.5, with an ideal lead, in which electrons travel without scattering, attached between two perfect reservoirs with electrochemical potentials μ_L and $\mu_R = \mu_L + eV$, where V is the applied voltage. And let T and R be the transmission and reflection probabilities respectively, of a scatterer between the ideal leads for the electrons at the Fermi level. Then the total current flowing across the system is given by

$$I = (-e) v_F \frac{\delta n}{\delta E} T(\mu_L - \mu_R) \quad , \tag{1.7}$$

where, $\delta n / \delta E = 2/h v_F$ is the density of states of the electrons, in unit length of wire moving from left to right. The factor 2 comes from spin degeneracy, and v_F is the

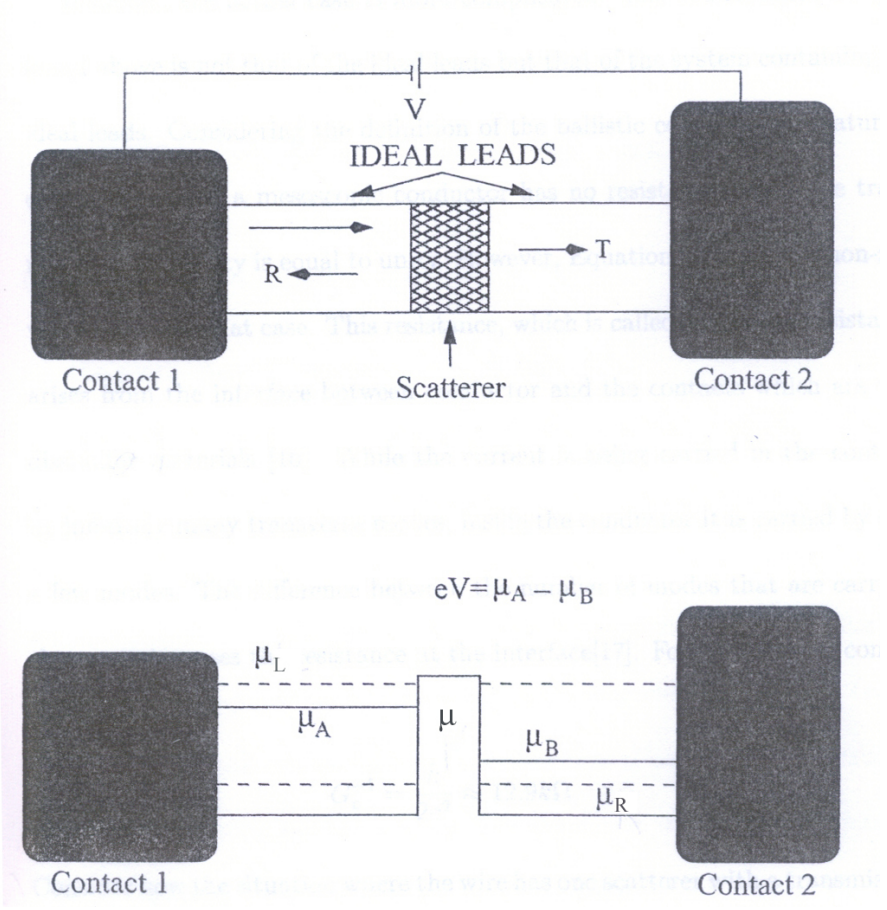

Figure 1.5: A conductor with one scatter having a transmission probability of T is connected between two large contacts through two leads, and this system can be reduced to the barrier problem.

Fermi velocity. Only the electrons with energies between μ_L and μ_R contribute to the net current since below both μ_L and μ_R currents from left and from right cancel each other. On the other hand, above both μ_L and μ_R there are no electrons and hence no current. Since the conductance is the ratio of the current to the voltage applied across the system and remembering that the voltage difference between L and R is

$$V_{RL} = \frac{\mu_L - \mu_R}{-e} \quad ,$$

the two terminal conductance can be written as

$$G = \frac{I}{V_{RL}} = \frac{2e^2}{h} T \quad . \tag{1.8}$$

It is important to note that with a suitable combination of the density of states and

the Fermi velocity, no quantity related to the energy band of the electrons appear in the final expression for the conductance, G.

The conductance formula $G = (2e^2/h)T$ definitely shows that scatterers give rise to resistance by reducing the transmission probability T. Intuitively this is satisfactory since we all perceive that the resistance of a sample ought to be related with which electrons can transmit through it. On the other hand, it arises some questions regarding the meaning of resistance on a microscopic scale. Considering the definition of the ballistic conductor, that is a conductor with no scattering, we naturally expect that such a mesoscopic conductor should have zero resistance. But Eq. (1.8) gives the nonzero value $h/2e^2$ for that case. This resistance, called as contact resistance, arises from the interface between the conductor and the contacts.[13] The conductor and the contacts are very dissimilar materials. The current is carried in the contacts by infinitely many transverse modes and inside the conductor it is carried by only one mode. This difference between the number of modes that are carrying the current causes the resistance at the interface. If T=1 contact resistance is

$$G_c^{-1} = \frac{h}{2e^2} \approx 12.9k\Omega.$$

For the case in Fig. 1.5 where the wire has one scatterer, the conductance is given by Eq. (1.8), as we have seen above. So the total resistance of this system is $R_{tot} = 1/G = h/(2e^2T)$, which is the sum of the contact resistance, G_c^{-1}, and the scatterer resistance, G_s^{-1};

$$\frac{1}{G} = \frac{h}{2e^2}\frac{1}{T} = G_c^{-1} + G_s^{-1}$$

Hence, the scatterer conductance becomes,

$$G_s = \frac{2e^2}{h}\frac{T}{1-T} = \frac{2e^2}{h}\frac{T}{R}$$

This formula is valid for single-channel case and is known as Landauer Formula. This equation is the original equation derived by Landauer.[11] However, Eq. (1.8) is used in applications since we are interested in the total conductance.[13, 14]

1.3 Büttiker's Model of Dephasing

Decoherence in particle transport can be simulated in several ways. [15, 16] Among the first was by Büttiker who considered an electron reservoir coupled by a lead to

a mesoscopic system as a phase breaker or inelastic scatterer (voltage probe). [17] Landauer's approach, which gives the conductance of an obstacle due to elastic scattering at the obstacle, is improved by including localized inelastic scatterers within the sample. The inelastic scatterers invoked include an electron reservoir coupled to the wire.

This approach has been widely used to investigate the effect of decoherence on conductance. This method which uses voltage probes as dephasors is interesting because of its conceptual clarity and its close relation to experiments.[17] It provides a useful trick to simulate lack of full coherence in transport properties. The major advantage of this method is that the effect of inelastic scattering can be studied by solving an elastic scattering problem.

Büttiker proposed a conceptually simple model to simulate the phase-breaking effect in partially coherent transport trough a mesoscopic system by coupling electron reservoirs to the conductor. The reservoir does not supply or draw a net current, but permits inelastic phase randomizing events.[17, 18, 19] He has investigated the resistance of a series of two obstacles and studied the transition from completely coherent transmission through the sample to completely incoherent transmission. By using a single reservoir to model a single dephasing scatterer he obtained that for a sample with a small transmission probability, increasing inelastic scattering decreases the resistance, and at an intermediate value of inelastic scattering, the resistance attains a minimum to increase again when inelastic scattering processes start to dominate the resistance.[17]

The model of an inelastic scatterer is shown in Fig. 1.6. The wire (channel 1 to the left and channel 2 to the right) is coupled via channels 3 and 4 to a reservoir. Carriers, which are scattered into channels 3 and 4 and incident in the reservoir, are absorbed regardless of their energy and phase. Moreover, the reservoir emits electrons into the adjacent conductor up to its chemical potential.[11, 12] Then the carriers are scattered inelastically in the reservoir and reemitted into channels 3 and 4 by the reservoir. During the tunnelling process, electron waves have certain probabilities of being scattered into the reservoir, undergoing phase randomization in it, then returning into the system via the coupler. Because of dephasing, the reemitted component does not interfere with that having not entered the reservoir.[17, 19]

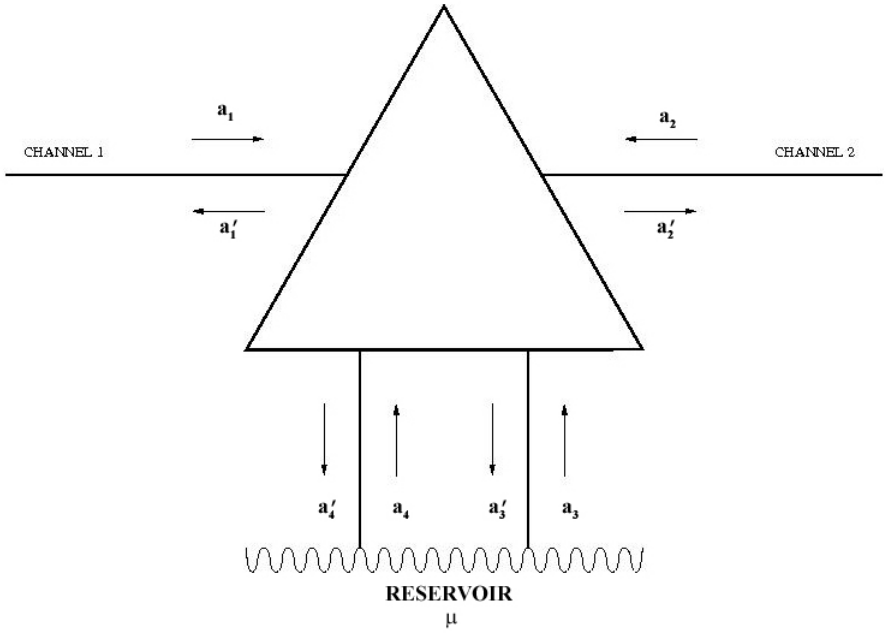

Figure 1.6: Model of inelastic scatterer.

The chemical potential μ will be specified such that the net current flow to the reservoir is zero. The chemical potential μ will be equal to the Fermi energy E_F at equilibrium, but when there exists current flow in the wire, μ will depend on the unequal distribution of left and right moving carriers.[9, 17] The coupler connecting wire to the reservoir is represented by an S matrix which determines the outgoing wave amplitudes $a' = (a'_1, a'_2, a'_3, a'_4)$ in terms of the incoming wave amplitudes $a = (a_1, a_2, a_3, a_4)$. A carrier in channel 1 reaching to the coupler has a probability $R_{11} = |S_{11}|^2$ to be reflected back into channel 1, a probability $T_{21} = |S_{21}|^2$ to be transmitted into channel 2, and probabilities $T_{31} = |S_{31}|^2$ and $T_{41} = |S_{41}|^2$ to be scattered into channels 3 and 4, respectively. A carrier emitted by the reservoir into channel 3 has a probability $R_{33} = |S_{33}|^2$ to be reflected back into channel 3, a probability $R_{43} = |S_{43}|^2$ to be reflected into channel 4, and has probabilities T_{13} and T_{23} to be transmitted into channels 1 and 2, respectively.

The phase of a carrier which is transmitted from channel 1 to channel 2 is not randomized since the carrier does not enter the reservoir. Consequently, the probability of a carrier incident from channel 1, i.e., from the left to traverse the sample

coherently is $T_{c,L} = T_{21}$. Similarly the proceeding of direct reflection is coherent and hence $R_{c,L} = R_{11}$ is the probability for coherent reflection of a carrier incident from the left. Likewise $T_{c,R} = T_{12}$ and $R_{c,R} = R_{22}$ are the coherent scattering probabilities for carriers arriving in channel 2, i.e., from the right. However, carriers which are transmitted from channel 3 or 4 into channel 1 or 2 have a phase which is not associated to that of the carriers incident in channels 1 and 2. Finally, Büttiker denoted the total probability of carriers from channels 3 and 4 to be scattered into channel 1 by

$$S_b = T_{13} + T_{14},$$

where S_b is the probability for incoherent backward scattering. And the probability of carriers from channel 3 and 4 to be transmitted into channel 2 by

$$S_f = T_{23} + T_{24},$$

where S_f is the probability for incoherent forward scattering. From current conservation we can say that scattering matrix S is unitary and in the absence of magnetic field also symmetric.[4] So we have $R_{11}+T_{12}+T_{13}+T_{14} = 1$ and $T_{21}+R_{22}+T_{23}+T_{24} = 1$, which become

$$R_{c,L} + T_c + S_b = 1,$$
$$T_c + R_{c,R} + S_f = 1$$

by using the definitions given above. Because of the symmetry $T_{21} = T_{12}$ the indices R and L on T_c have been dropped in here.

At that point Büttiker applied Landauer's concept to obtain the conductance of a sample with a single inelastic scatterer. A current is imposed to the wire by connecting it to two reservoirs, which are acting as a source and sink of carriers. Left-hand side (LHS) reservoir feeds carriers with positive velocity into the wire up to a quasi Fermi energy μ_L. And the right-hand side (RHS) reservoir feeds carriers with negative velocity into the wire up to a quasi Fermi energy μ_R. Lastly, the scatterer feeds the channels up to a Fermi energy μ which remains to be determined in order to obtain a zero current flow to the reservoir. It is assumed that $\mu_L > \mu > \mu_R$. All channels are full for energies smaller than μ_R, so we only need to consider the energy range between μ_R and μ_L.[17, 18] Injected current into the wire by the reservoir on the LHS

is

$$I_{in} = e\upsilon(\frac{dn}{dE})(\mu_L - \mu_R) = \frac{e}{2\Pi\hbar}(\mu_L - \mu_R)$$

Here $\frac{dn}{dE} = \frac{2}{h\upsilon}$ has been used as the density of states for the particles with positive velocity in a one-dimensional wire, the factor 2 comes from spin degeneracy. It is assumed that the density of states is the same in all channels. The reservoir in Figure 1.6 of the scatterer emits a current,

$$I_s = (\frac{2e}{h})(\mu - \mu_R)$$

into channels 3 and 4. Now consider the net currents flows in channels 1 and 4. The current in channel 1 is

$$I_1 = \frac{2e}{h}[(1 - R_{11})(\mu_L - \mu_R) - S_b(\mu - \mu_R)]$$

where R_{11} is the probability of carriers coming from channel 1 to be reflected back into channel 1, and the last term shows the contribution of the carrier flux from the carriers that are emitted by the reservoir in the backward direction. Likewise in channel 2 the current is

$$I_2 = \frac{2e}{h}[T_{21}(\mu_L - \mu_R) + S_f(\mu - \mu_R)]$$

where S_f is the probability for forward scattering. Finally, for the current in the lead which is coupling the wire to the reservoir we have

$$I_3 = \frac{2e}{h}[(1 - R_{33} - R_{34})(\mu - \mu_R) - T_{31}(\mu_L - \mu_R)]$$

and

$$I_4 = \frac{2e}{h}[(1 - R_{44} - R_{43})(\mu - \mu_R) - T_{41}(\mu_L - \mu_R)]$$

where R_{34} stands for the probability of a carrier in channel 4 for reflection at the coupler into channel 3, and vice versa. The chemical potential μ is specified by the requirement that no net current flows into the reservoir. So we have

$$I_3 + I_4 = 0$$

Yielding μ as

$$\mu = \mu_R + \chi(\mu_L - \mu_R)$$

where

$$\chi = \frac{S_b}{S_b + S_f}$$

To get χ the unitary relations $T_{14}+T_{24}+R_{34}+R_{44}=1$ and $T_{13}+T_{23}+R_{33}+R_{43}=1$ and the symmetry of the reflection and transmission probabilities, $T_{ij}=T_{ji}$ and $R_{ij}=R_{ji}$ have been used. With use of these symmetry relations and $S_b=T_{13}+T_{14}$, we see that the current is indeed conserved $I_1=I_2=I$, with

$$I=\frac{2e}{h}(T_{21}+\chi S_f)(\mu_L-\mu_R),$$

So the conductance G is expressed as

$$G=\frac{I}{V}=\frac{2e^2}{h}(T_{21}+\chi S_f)$$

since $\mu_L-\mu_R=eV$.

1.4 Our Model

We are interested in extending Büttiker's model for decoherence in 1D transport in a way that decoherence proceeds at every location. In Chapter 2 we introduce our geometry of the problem. The incoherent transmission is calculated from Büttiker's voltage probe model, by mapping the three probe Büttiker's method into an N probe geometry. In Chapter 3 we reveal our results and conclusions.

Our model is more consistent with the prevalent notions of decoherence since the placement of the single scatterer in Büttiker's model effects the electron transmission. In Chapter 3 we show the details about this comparison.

CHAPTER 2

A CONTINUUM MODEL FOR DECOHERENCE

2.1 Geometry of the Model

We are interested in extending Büttiker's model for decoherence in 1D transport in a way that decoherence proceeds at every location. The geometry of the problem is shown in Fig. 2.1. Here there is a "main line" along which electrons move and scatter. Apart from that, N additional lines are also placed for modelling the decoherence effects on the main line. It is assumed that the electrons can jump between the main line and the additional ones. It can go to equilibrium in those lines but will eventually return back and at the end coherence with the wavefunction in the main line will be lost.

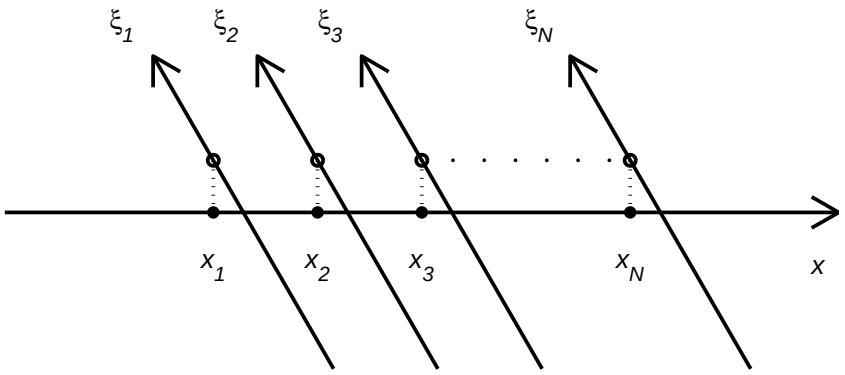

Figure 2.1: The geometry of the problem.

2.2 Hamiltonian of the System

Before writing down the Hamiltonian of the whole system, we describe the possible states of the electrons first. The state of electron at position x on the main line is denoted by $|x\rangle$. The state when the electron is on line-j at the position ξ will be denoted by $|\xi, j\rangle$. All of these are distinct states. Moreover, any state $|\psi\rangle$ can be expressed as a superposition of these as

$$|\psi\rangle = \int dx \psi(x) |x\rangle + \sum_j \int d\xi \phi_j(\xi) |\xi, j\rangle \quad , \tag{2.1}$$

where $\psi(x)$ will be called the wavefunction on the main line and $\phi_j(x)$ will be called the wavefunction on line-j. If the state $|\psi\rangle$ is normalizable, we have the following

$$\langle\psi|\psi\rangle = \int dx |\psi(x)|^2 + \sum_j \int d\xi |\phi_j(\xi)|^2 \quad .$$

Next, we write a possible Hamiltonian for the electrons. First note that the electrons should have the normal behavior on each of the lines when all other lines are forgotten about. We will suppose that on the main line, the electron moves under a potential $V(x)$. On the the additional lines, it will be assumed to be free, moving under a constant potential. We will denote those Hamiltonians of the main and additional lines by h_0 and h_j respectively. We can write down the following differential and abstract representations of these operators

$$\begin{aligned} h_0 &= -\tfrac{\hbar^2}{2m^*}\tfrac{d^2}{dx^2} + V(x) \quad , \quad h_0 = \int\int dx dx' h_0(x;x') |x\rangle \langle x'| \quad , \\ h_j &= -\tfrac{\hbar^2}{2m^*}\tfrac{d^2}{d\xi^2} + V_j \quad , \quad h_j = \int\int d\xi d\xi' h_j(\xi;\xi') |\xi, j\rangle \langle \xi', j| \quad . \end{aligned}$$

Note that these operators act on their respective spaces. As a result, we have $h_0 |\xi, j\rangle = h_j |x\rangle = 0$. Also $h_j |\xi, i\rangle = 0$ if $i \neq j$. As a result, for the state given in Eq. (2.1) we have

$$\begin{aligned} h_0 |\psi\rangle &= \int dx \left(-\frac{\hbar^2}{2m^*} \frac{d^2\psi(x)}{dx^2} + V(x)\psi(x) \right) |x\rangle \quad , \\ h_j |\psi\rangle &= \int d\xi \left(-\frac{\hbar^2}{2m^*} \frac{d^2\phi_j(\xi)}{d\xi^2} + V_j\phi_j(\xi) \right) |\xi, j\rangle \quad . \end{aligned}$$

Next, we add a term for the transfer of electrons between lines. We will assume that when the electron is at position x_j on the main line, it can jump to the origin, $\xi = 0$, of line-j. A term in the Hamiltonian of the form $|\xi = 0, j\rangle \langle x_j|$ handles this.

The hermitian conjugate handles the opposite process, namely jumping from line-j to the main line. We will write the Hamiltonian as

$$H = h_0 + \sum_j h_j + \sum_j g_j \left(|\xi = 0, j\rangle \langle x_j| + |x_j\rangle \langle \xi = 0, j| \right) \quad .$$

Here g_j is a real number representing the coupling strength to line-j. It could have been chosen complex valued, but this is unnecessary since it does not introduce any new effects. Moreover, the reality implies a simple time-reversal operation (complex conjugation of wavefunction) and the symmetry implies that the scattering matrix is symmetric.

2.3 The Schrödinger's Equation and The Solution of the Wavefunction

The Schrödinger's equation, $H|\psi\rangle = E|\psi\rangle$ can be expressed in terms of wavefunctions as

$$\left(-\frac{\hbar^2}{2m^*} \frac{d^2\psi(x)}{dx^2} + V(x)\psi(x) \right) + \sum_j g_j \phi_j(0) \delta(x - x_j) = E\psi(x) \quad , \tag{2.2}$$

$$\left(-\frac{\hbar^2}{2m^*} \frac{d^2\phi_j(\xi)}{d\xi^2} + V_j \phi_j(\xi) \right) + g_j \psi(x_j) \delta(\xi) = E\phi_j(\xi) \quad . \tag{2.3}$$

We will write down the solutions of this equation below.

Obviously we will be interested only in extended solutions. And for these, we are going to be interested in the behavior of the wavefunctions far from the scattering region. We will assume that the potential on the main line, $V(x)$, is constant outside a certain interval.

$$V(x) = \begin{cases} V_L & \text{for } x < x_L^{(b)} \\ V_R & \text{for } x > x_R^{(b)} \end{cases}$$

where between the points $x_L^{(b)}$ and $x_R^{(b)}$, $V(x)$ varies. The scattering region and the points x_j are contained in this interval. For any energy E, the left and right wavenumbers will be defined as

$$k_L = \sqrt{\frac{2m^*(E - V_L)}{\hbar^2}} \quad , \qquad k_R = \sqrt{\frac{2m^*(E - V_R)}{\hbar^2}} \quad .$$

For the line-j, the electrons move freely with wavenumbers

$$k_j = \sqrt{\frac{2m^*(E - V_j)}{\hbar^2}} \quad .$$

The corresponding velocities are defined accordingly, $v_L = \hbar k_L/m^*$ etc.

We will define the incoming wave amplitudes a_j, a'_j and the outgoing wave amplitudes b_j, b'_j ($j = 0, 1, \ldots, N$) for any solution at energy E by

$$\begin{aligned}
\psi(x) &= \begin{cases} \frac{1}{\sqrt{v_L}}\left(a_0 e^{ik_L x} + b_0 e^{-ik_L x}\right) & \text{for } x < x_L^{(b)} \\ \frac{1}{\sqrt{v_R}}\left(a'_0 e^{-ik_R x} + b'_0 e^{ik_R x}\right) & \text{for } x > x_R^{(b)} \end{cases} \\
\phi_j(\xi) &= \frac{1}{\sqrt{v_j}} \begin{cases} a_j e^{ik_j \xi} + b_j e^{-ik_j \xi} & \text{for } \xi < 0 \\ a'_j e^{-ik_j \xi} + b'_j e^{ik_j \xi} & \text{for } \xi > 0 \end{cases}
\end{aligned}$$

There are $2N+2$ independent solutions of the wave equation. Any particular solution can be obtained by choosing arbitrary values for the incoming wave amplitudes a_j and a'_j. From these values alone, the outgoing wave amplitudes b_j and b'_j can be determined. The relation between the outgoing and incoming amplitudes involves the scattering matrix

$$\begin{aligned}
b_j &= \sum_{i=0}^{N} S_{ji} a_i + S_{ji'} a'_i \quad , \\
b'_j &= \sum_{i=0}^{N} S_{j'i} a_i + S_{j'i'} a'_i \quad .
\end{aligned}$$

Our purpose is to obtain the scattering matrix. Through this we can calculate the transport properties of the system.

2.3.1 Solution for line-j

First we write down the solution of the Schrödinger's equation for line-j. The wavefunction $\phi_j(\xi)$ is continuous at the origin $\xi = 0$,

$$\phi_j(0+) = \phi_j(0-),$$

$$a_j + b_j = a'_j + b'_j. \tag{2.4}$$

But its derivative has a discontinuity

$$\Delta\phi'_j(0) = \phi'_j(0+) - \phi'_j(0-) = \frac{2m^* g_j}{\hbar^2}\psi(x_j) \quad .$$

$$b'_j + b_j = a_j + a'_j - 2i\frac{g_j}{\hbar\sqrt{v_j}}\psi(x_j). \tag{2.5}$$

Then by adding and subtracting Eq. (2.4) and Eq. (2.5) we get the outgoing amplitudes as

$$b'_j = a_j - i\gamma_j\psi(x_j) \quad , \tag{2.6}$$

$$b_j = a'_j - i\gamma_j\psi(x_j) \quad , \tag{2.7}$$

where

$$\gamma_j = \frac{g_j}{\hbar\sqrt{v_j}} \quad . \tag{2.8}$$

Since g_j has dimensions Energy$\times$Length, γ_j has the dimensions of square root of velocity. We will need the following expression below.

$$\phi_j(0) = \frac{a_j + b_j}{\sqrt{v_j}} = \frac{a'_j + b'_j}{\sqrt{v_j}}$$

by putting b'_j from Eq. (2.6) we get

$$\phi_j(0) = \frac{a'_j + a_j - i\gamma_j\psi(x_j)}{\sqrt{v_j}}$$

Then

$$\phi_j(0) = -\frac{i}{\sqrt{v_j}}\left(\gamma_j\psi(x_j) + i(a_j + a'_j)\right) = -\frac{i}{\sqrt{v_j}}\theta_j \quad . \tag{2.9}$$

2.3.2 Solution for the main line

Schrödinger's equation for the main line, from Eq. (2.2), can be expressed as

$$[E - h_0]\psi(x) = \sum_j g_j\phi_j(0)\delta(x - x_j) = -i\hbar\sum_j \gamma_j\theta_j\delta(x - x_j) \quad .$$

Equations of this form can be solved easily by using the Green function as

$$\psi(x) = \psi_0(x) + \int dy G(x;y)\left(-i\hbar\sum_j \gamma_j\theta_j\delta(x - x_j)\right) \quad , \tag{2.10}$$

where ψ_0 is a particular solution of the homogeneous equation, $[E - h_0]\psi_0 = 0$, and $G(x;y)$ is the Green function satisfying

$$[E - h_0(x)]G(x;y) = \delta(x - y) \quad .$$

First, the general solution of the homogeneous equation can be expressed as a superposition of two scattering solutions, $\varphi_L(x,E)$ and $\varphi_R(x,E)$, of the main line.

These solutions satisfy

$$\varphi_L(x,E) = \begin{cases} \frac{1}{\sqrt{v_L}}\left(e^{ik_Lx} + r_0 e^{-ik_Lx}\right) & \text{for } x < x_L^{(b)} \\ \frac{1}{\sqrt{v_R}}\, t_0 e^{ik_Rx} & \text{for } x > x_R^{(b)} \end{cases}$$

$$\varphi_R(x,E) = \begin{cases} \frac{1}{\sqrt{v_L}}\, t_0' e^{-ik_Lx} & \text{for } x < x_L^{(b)} \\ \frac{1}{\sqrt{v_R}}\left(e^{-ik_Rx} + r_0' e^{ik_Rx}\right) & \text{for } x > x_R^{(b)} \end{cases}$$

These are the solutions of $[h_0 - E]\varphi_{L,R} = 0$ obtained when there are no additional lines. Here r_0, r_0', t_0 and t_0' are reflection and transmission amplitudes and we have $t_0 = t_0'$ due to the symmetry of the scattering matrix.

Green functions can be expressed in terms of these solutions, $\varphi_{L,R}$. We will be interested only in $G^{(+)}$, the retarded Green function (due to the reason explained below). The function is symmetric in its arguments, $G^{(+)}(x;y) = G^{(+)}(y;x)$. When $x \neq y$, the wave equation is satisfied for both arguments. Using this, we can write the following general solution (say for $x < y$),

$$G^{(+)}(x;y) = (\alpha\varphi_L(x) + \beta\varphi_R(x))(\mu\varphi_L(y) + \nu\varphi_R(y)) \quad .$$

For the retarded Green function $G^{(+)}$, we want the expressions involving only outgoing waves at their respective regions. For this reason we set $\alpha = \nu = 0$. (The normal definition is this: When energy E is moved off from the real axis to the upper complex plane, $E \to E + i\epsilon$, the Green function should remain finite at infinities.) In any case, using the symmetry we get the following for any x and y

$$G^{(+)}(x;y) = A\varphi_R(x_<)\varphi_L(x_>) = \begin{cases} A\varphi_R(x)\varphi_L(y) & \text{for } x < y \\ A\varphi_R(y)\varphi_L(x) & \text{for } x > y \end{cases}$$

The constant A in front can be calculated by using the discontinuity of x-derivative at $x = y$.

$$\frac{\hbar^2}{2m^*}\left(\frac{\partial G^{(+)}(x;y)}{\partial x}\bigg]_{x=y+0} - \frac{\partial G^{(+)}(x;y)}{\partial x}\bigg]_{x=y-0}\right) = 1$$

This gives

$$A(\varphi_L'(y)\varphi_R(y) - \varphi_R'(y)\varphi_L(y)) = \frac{2m^*}{\hbar^2} \quad ,$$

where the terms inside the parentheses is the constant Wronskian. Calculation of this at the left $x = y < x_L^{(b)}$ gives $A = -i/\hbar t_0$.

$$G^{(+)}(x;y) = -\frac{i}{\hbar t_0}\varphi_R(x_<)\varphi_L(x_>) \quad . \tag{2.11}$$

The solution of the wavefunction on the main line can now be written down. First note that in Eq. (2.10), the term containing the Green function can have only outgoing waves if $G^{(+)}$ is used. In that case, all incoming waves should appear in ψ_0. As a result we have $\psi_0 = a_0\varphi_L + a'_0\varphi_R$. The wavefunction $\psi(x)$ is

$$\psi(x) = a_0\varphi_L(x) + a'_0\varphi_R(x) - i\hbar\sum_j G^{(+)}(x;x_j)\gamma_j\theta_j \quad .$$

Since θ_j depends on $\psi(x_j)$ (Eq. (2.9)), we need to solve this equation. To simplify the notation we first define θ_{0j} as

$$\theta_{0j} = \gamma_j\psi_0(x_j) + i(a_j + a'_j) \quad ,$$

and note that θ_{0j} depends only on incoming wave amplitudes. Using this, we get the following set of N equations,

$$\theta_\ell = \theta_{0\ell} - i\hbar\sum_j \gamma_\ell G^{(+)}(x_\ell,x_j)\gamma_j\theta_j \quad .$$

Let us now define an $N\times N$ matrix $\Gamma_{\ell j}$ as

$$\begin{aligned}
\Gamma_{\ell j} &= \delta_{\ell j} + i\hbar\gamma_\ell G^{(+)}(x_\ell,x_j)\gamma_j = \delta_{\ell j} + \frac{\gamma_\ell\gamma_j}{t_0}\varphi_R(x_{j_<})\varphi_L(x_{j_>}) \\
&= \delta_{\ell j} + \frac{1}{t_0}f_{Rj_<}f_{Lj_>} \quad , \\
\text{where} \qquad & f_{Rj} = \gamma_j\varphi_R(x_j) \quad , \qquad f_{Lj} = \gamma_j\varphi_L(x_j)
\end{aligned}$$

The final solution is $\theta_j = \sum_\ell \left(\Gamma^{-1}\right)_{j\ell}\theta_{0\ell}$ from which we will obtain all scattering amplitudes. The inverse of Γ, has a very simple form (this is shown in Appendix A) which is

$$\left(\Gamma^{-1}\right)_{\ell j} = \delta_{\ell j} - \frac{1}{t_d}\, q_{Rj_<}\, q_{Lj_>} \quad ,$$

where

$$q_L = \Gamma^{-1}f_L \quad , \quad q_R = \Gamma^{-1}f_R \quad , \quad t_d = t_0 - f_R^T\Gamma^{-1}f_L \quad .$$

2.4 The scattering matrix of the system

First look at the behavior of $\psi(x)$ for $x < x_L^{(b)}$.

$$\begin{aligned}
\psi(x) &= \psi_0(x) - i\hbar \sum_{j\ell} G^{(+)}(x; x_j)\gamma_j \left(\Gamma^{-1}\right)_{j\ell} \theta_{0\ell} \\
&= a_0\varphi_L(x) + a_0'\varphi_R(x) - \frac{1}{t_0}\varphi_R(x) \sum_{j\ell} f_{Lj} \left(\Gamma^{-1}\right)_{j\ell} \theta_{0\ell} \\
&= a_0\varphi_L(x) + \left(a_0' - \frac{1}{t_0}\sum_{\ell} q_{L\ell}\theta_{0\ell}\right)\varphi_R(x) \\
&= \frac{1}{\sqrt{v_L}} a_0 e^{ik_L x} + \frac{1}{\sqrt{v_L}} \left(r_0 a_0 + t_0 a_0' - \sum_{\ell} q_{L\ell}\theta_{0\ell}\right) e^{-ik_L x}
\end{aligned}$$

Therefore we have

$$b_0 = r_0 a_0 + t_0 a_0' - \sum_{\ell} q_{L_\ell}\theta_{0\ell} \quad .$$

We do the same thing for $x > x_R^{(b)}$ and in this case we get

$$b_0' = t_0 a_0 + r_0' a_0' - \sum_{\ell} q_{R_\ell}\theta_{0\ell} \quad .$$

The equations (2.6,2.7) give us the outgoing amplitudes at the additional lines as follows

$$b_j = -a_j - i\left(\Gamma^{-1}\right)_{j\ell}\theta_{0\ell} \quad , \qquad b_j' = -a_j' - i\left(\Gamma^{-1}\right)_{j\ell}\theta_{0\ell}$$

Finally, $\theta_{0\ell}$ depends only on the incoming wave amplitudes through

$$\theta_{0\ell} = a_0 f_{L\ell} + a_0' f_{R\ell} + i(a_\ell + a_\ell') \quad .$$

From these expressions we can read off the scattering matrix elements as follows. First scattering amplitudes for the main line

$$t_d = S_{LR} = S_{RL} = t_0 - f_L^T \Gamma^{-1} f_R = t_0 - q_L^T f_R = t_0 - q_R^T f_L \quad , \tag{2.12}$$

$$S_{LL} = r_0 - f_L^T \Gamma^{-1} f_L = r_0 - q_L^T f_L \quad , \tag{2.13}$$

$$S_{RR} = r_0' - f_R^T \Gamma^{-1} f_R = r_0' - q_R^T f_R \quad . \tag{2.14}$$

We will use the symbol t_d for the amplitude S_{LR} and call it the direct transmission

amplitude. For the scattering into and between the additional lines we have

$$S_{Lj} = S_{Lj'} = S_{jL} = S_{j'L} = -iq_{Lj} \quad , \tag{2.15}$$

$$S_{Rj} = S_{Rj'} = S_{jR} = S_{j'R} = -iq_{Rj} \quad , \tag{2.16}$$

$$S_{j\ell} = S_{j'\ell'} = -\delta_{j\ell} + \left(\Gamma^{-1}\right)_{j\ell} \quad , \tag{2.17}$$

$$S_{j\ell'} = S_{j'\ell} = \left(\Gamma^{-1}\right)_{j\ell} \quad . \tag{2.18}$$

Note that j and j' denote the negative and positive axes respectively on line-j. These two directions are entirely equivalent for scattering. Therefore if an inversion is taken on line-j (i.e., j is switch with j') then the scattering matrix should remain invariant. This symmetry can be seen in the expressions above.

For example, for the scattering between two different additional lines j and ℓ ($j \neq \ell$), the scattering amplitude is

$$-\frac{1}{t_d}\, q_{Rj_<}\, q_{Lj_>}$$

independent of the directions the wave comes and goes. If a wave coming from line-j is scattered back into the same line (perhaps through passing to the main line) then the transmission amplitude is

$$(\Gamma^{-1})_{jj} = 1 - \frac{1}{t_d} q_{Lj} q_{Rj}$$

and the reflection amplitude is

$$-1 + (\Gamma^{-1})_{jj} = -\frac{1}{t_d} q_{Lj} q_{Rj}$$

Note also that the S-matrix has to be unitary. [4] An interesting question is this: Which properties should the Γ matrix satisfy so that the resultant S-matrix is unitary? It appears that the following equations

$$\varphi_L(x)^* = r_0^* \varphi_L(x) + t_0^* \varphi_R(x) \quad ,$$

$$\varphi_R(x)^* = t_0^* \varphi_L(x) + r_0'^* \varphi_R(x) \quad ,$$

which are also satisfied by f_L and f_R, are the only ones we need. From here, it can be shown that Γ-matrix and its inverse satisfy

$$\Gamma + \Gamma^\dagger - 2I = f_L f_L^\dagger + f_R f_R^\dagger \quad ,$$

$$\Gamma^{-1} + (\Gamma^\dagger)^{-1} - 2\Gamma^{-1}(\Gamma^\dagger)^{-1} = q_L q_L^\dagger + q_R q_R^\dagger \quad .$$

Unitarity of S-matrix follows from these.

2.5 Probabilities of the system

We will be using mostly the transmission probabilities. The direct transmission probability is $T_d = |t_d|^2$. The transmission probability from left lead to a direction in line-j and the corresponding quantity for the right lead are

$$\begin{aligned} T_{Lj} &= |q_{Lj}|^2 \quad , \\ T_{Rj} &= |q_{Rj}|^2 \quad . \end{aligned}$$

The transmission probabilities between two different lines j and ℓ can be expressed in terms of the quantities above

$$T_{j\ell} = \left| \frac{1}{t_d}\, q_{Rj<}\, q_{Lj>} \right|^2 = \frac{T_{Rj<}\, T_{Lj>}}{T_d} \quad .$$

In other words, knowing the transmission probabilities for the main line, we can determine these probabilities between the additional lines.

2.6 Conductance of the system

Suppose that the leads of the main line have electrostatic potentials W_L and W_R. We are going to assume that both directions on the additional lines are at the same potential W_j. The differences in chemical potentials are related to these potentials by $\mu_L - \mu_R = (-e)(W_L - W_R)$ etc.

The current that enters from the lead α and go to the lead β can be expressed as

$$I_{\alpha\to\beta} = 2\frac{(-e)}{h}(\mu_\alpha - \mu_\beta) = \frac{2e^2}{h}(W_\alpha - W_\beta) = G_0(W_\alpha - W_\beta) \quad ,$$

where G_0 is the conductance quantum. Form these we can get expressions for the total current going into a lead.

$$\begin{aligned} I_L &= G_0 \left[T_d(W_L - W_R) + \sum_j 2T_{Lj}(W_L - W_j) \right] \quad , \\ I_R &= G_0 \left[T_d(W_R - W_L) + \sum_j 2T_{Rj}(W_R - W_j) \right] \quad , \\ I_j = I_{j'} &= G_0 \big[T_{Lj}(W_j - W_L) + T_{Rj}(W_j - W_R) + T_{jj'}(W_j - W_j) \\ &\qquad + \sum_{\ell\neq j} 2T_{\ell j}(W_j - W_\ell) \Big] \quad , \end{aligned}$$

The total current going in has to be zero: $I_L + I_R + \sum_j 2I_j = 0$. Also, all the potentials W_α can be shifted by a constant amount, $W_\alpha \to W_\alpha + \delta W$, and this does not change the value of currents. Due to this we can choose one of the potentials (such as W_R) to be 0 (grounding).

Since additional lines are only imaginary, we require them to carry no current, $I_j = 0$. In this way, if electrons go into one of these lines, same number of electrons come back. In that case we have $I_L = -I_R = I$, the current passing from the device. We will suppose that $W_R = 0$ and express all other potentials in terms of W_L.

The equation that expresses that the current entering into line-j being zero is

$$T_{Lj} W_L = \left(T_{Lj} + T_{Rj} + 2 \sum_{\ell \neq j} T_{\ell j} \right) W_j - 2 \sum_{\ell \neq j} T_{j\ell} W_\ell \quad .$$

The terms inside the parentheses is equal to (by the unitarity of S-matrix)

$$1 - |S_{jj}|^2 - \left|S_{jj'}\right|^2 = \left(\frac{q_{Lj} q_{Rj}}{t_d} \right) + \left(\frac{q_{Lj} q_{Rj}}{t_d} \right)^* - 2 \frac{T_{Lj} T_{Rj}}{T_d} = m_j - 2 \frac{T_{Lj} T_{Rj}}{T_d} \quad .$$

We are going to define a new $N \times N$ matrix, P, with

$$P_{j\ell} = m_j \delta_{j\ell} - 2 \frac{T_{Rj_<} T_{Lj_>}}{T_d} \quad .$$

It is a symmetric matrix with real elements which also satisfies (because of the way the diagonal elements are defined)

$$\sum_\ell P_{j\ell} = T_{Lj} + T_{Rj} \quad .$$

Using this matrix, we can find the potentials W_j,

$$\frac{W_j}{W_L} = \sum_\ell P^{-1}_{j\ell} T_{L\ell} \quad .$$

Using these, the dimensionless conductance can be expressed as

$$\begin{aligned} g &= \frac{I}{G_0 W_L} \\ &= T_d + 2 \sum_j T_{Lj} - 2 \sum_{j\ell} T_{Lj} P^{-1}_{j\ell} T_{L\ell} \\ &= T_d + 2 \sum_{j\ell} T_{Rj} P^{-1}_{j\ell} T_{L\ell} \end{aligned}$$

2.7 The continuum version

We are now going to pass from the discrete model solved above to a continuum model where the additional lines are infinite in number and they are distributed uniformly to every position. Still, we may want to keep a finite range for the positions where these lines are in contact with the main line. For this reason, we will suppose that the region where decoherence occurs is on the interval between positions x_L^D and x_R^D.

Second, we are going to make a connection with the previous discrete problem. So, we are going to select N points uniformly within the decoherence interval.

$$x_L^D \leq x_1 < x_2 < \cdots < x_N \leq x_R^D \quad .$$

We are not going to specify how these points are chosen, but in $N \to \infty$ limit, they should fill out the whole interval. Let Δx_j be the length of interval where the point x_j corresponds to. A possible choice might be $\Delta x_j = x_{j+1} - x_j$ and $\Delta x_N = x_R^D - x_N$ if $x_1 = x_L^D$. Another possibility is choosing x_j in the middle of each subinterval of length Δx_j. In all cases, we should have $\sum \Delta x_j = (x_R^D - x_L^D)$.

We are going to define g_j, the coupling strength to line-j, by

$$g_j = g(x_j)\sqrt{\Delta x_j} \quad , \tag{2.19}$$

where $g(x)$ is a real function defined on the decoherence interval. It has dimensions of Energy$\times$Length$^{1/2}$. Similarly, the potential of line-j, V_j, has to be chosen as a continuous function of position of contact, x_j. Let $\hat{V}(x)$ denote this function, i.e., $V_j = \hat{V}(x_j)$. The velocity at line-j, v_j, will then be

$$v_j = v(x_j) = \sqrt{2(E - \hat{V}(x_j))/m^*} \quad .$$

Then we will define $\gamma(x)$ function as

$$\gamma(x) = \frac{g(x)}{\hbar\sqrt{v(x)}} \quad ,$$

and the coefficients γ_j becomes $\gamma(x_j)\sqrt{\Delta x_j}$. For this reason, the function $\gamma(x)$ has the dimensions of Time$^{-1/2}$.

It is natural to define the two functions $f_L(x)$ and $f_R(x)$ as

$$f_L(x) = \frac{g(x)\varphi_L(x)}{\hbar\sqrt{v(x)}} \quad , \qquad f_R(x) = \frac{g(x)\varphi_R(x)}{\hbar\sqrt{v(x)}} \quad .$$

In that case we have $f_{Lj} = f_L(x_j)\sqrt{\Delta x_j}$ and $f_{Rj} = f_R(x_j)\sqrt{\Delta x_j}$. The functions $f_{L,R}(x)$ have the dimensions Length$^{-1/2}$, but $f_{L,Rj}$ are dimensionless.

The Γ matrix is defined in the usual way as

$$\Gamma_{j\ell} = \delta_{j\ell} + \frac{1}{t_0} f_{Rj_<} f_{Lj_>} = \delta_{j\ell} + \frac{1}{t_0} f_R(x_{j_<}) f_L(x_{j_>}) \sqrt{\Delta x_j \Delta x_\ell}$$

We are interested in obtaining a functional form for the Γ matrix. Note that in discrete form, Γ^{-1} is applied to the vectors which have $\sqrt{\Delta x}$ factors in all of their elements. For this reason, let us investigate the general relation $a_j = \Gamma_{j\ell}\, b_\ell$ where $a_j = a(x_j)\sqrt{\Delta x_j}$ and $b_j = b(x_j)\sqrt{\Delta x_j}$.

$$a(x_j)\sqrt{\Delta x_j} = b(x_j)\sqrt{\Delta x_j} + \frac{\sqrt{\Delta x_j}}{t_0} \sum_\ell f_R(x_<) f(x_>)\, b(x_\ell) \Delta x_\ell \quad .$$

Eliminating the common factors in square roots we get a functional equation

$$a(x) = \int \Gamma(x;y) b(y) dy \quad ,$$

where

$$\Gamma(x;y) = \delta(x-y) + \frac{1}{t_0} f_R(x_<) f_L(x_>) \quad . \tag{2.20}$$

Therefore we are going to define functions $q_L(x)$ and $q_R(x)$ (defined only on the decoherence interval) by

$$f_{L,R}(x) = \int \Gamma(x;y) q_{L,R}(y) dy \quad . \tag{2.21}$$

Using these we have $q_{Lj} = q_L(x_j)\sqrt{\Delta x_j}$ etc. Similarly the inverse of Γ function can be expressed as

$$\Gamma^{-1}(x;y) = \delta(x-y) - \frac{1}{t_d} q_R(x_<) q_L(x_>) \quad ,$$

where

$$t_d = t_0 - \sum_j q_{Rj} f_{Lj} = t_0 - \int q_R(x) f_L(x) dx \quad .$$

The reflection amplitudes can also be expressed in the same form.

The transmission probabilities are

$$T_{Lj} = |q_L(x_j)|^2 \Delta x_j = T_L(x_j) \Delta x_j \quad , \qquad T_{Rj} = |q_R(x_j)|^2 \Delta x_j = T_R(x_j) \Delta x_j \quad .$$

It is good that the probabilities turn out to be proportional to the interval length. Note that the line-j takes care of the decoherence on that interval. The transmission between two different intervals

$$T_{j\ell} = \frac{|q_R(x_<)|^2 \, |q_R(x_>)|^2}{T_d} \Delta x_j \Delta x_\ell = \frac{T_R(x_<)\, T_L(x_>)}{T_d} \Delta x_j \Delta x_\ell$$

is also proportional to both of the lengths of the corresponding intervals.

Next, note that

$$m_j = 2\,\mathrm{Re}\,\frac{q_R(x_j)q_L(x_j)}{t_d}\;\Delta x_j = M(x_j)\Delta x_j \quad .$$

The matrix elements of P becomes

$$P_{j\ell} = \delta_{j\ell}M(x_j)\Delta x_j - 2\frac{T_R(x_<)T_L(x_>)}{T_d}\Delta x_j\Delta x_\ell \quad .$$

This matrix looks different from Γ in the way it contains interval lengths. But still we can define a function form

$$P(x;y) = M(x)\delta(x-y) - 2\frac{T_R(x_<)T_L(x_>)}{T_d} \quad .$$

So, if $W(x_j)$ denotes the electrostatic potential on line-j, we have

$$T_L(x) = \int P(x;y)\frac{W(y)}{W_L}dy \quad .$$

$P(x;y)$ also satisfies the equation

$$\int P(x;y)dy = T_L(x) + T_R(x) \quad .$$

Finally, it can be shown that the dimensionless conductance g can be expressed as

$$\begin{aligned} g &= \frac{I}{G_0 W_L} \\ &= T_d + 2\int T_L(x)dx - 2\int\int T_L(x)P^{-1}(x;y)T_L(y)dxdy \\ &= T_d + 2\int\int T_R(x)P^{-1}(x;y)T_L(y)dxdy \end{aligned}$$

where $P^{-1}(x;y)$ is the inverse of $P(x;y)$

$$\int P^{-1}(x;y)P(y;z)dy = \delta(x-z) \quad .$$

2.8 Small decoherence rate

In here we will assume that the coupling strength expression $g(x)$ is small, so that we can expand all relevant quantities in $g(x)$. Mostly we will be interested in the lowest order term. The functions f_L and f_R are of first order in g. The Γ function-matrix is

$$\Gamma(x;y) = \delta(x-y) + \frac{1}{t_0}f_R(x_<)f_L(x_>) \quad , \qquad \Gamma^{-1}(x;y) \approx \delta(x-y) - \frac{1}{t_0}f_R(x_<)f_L(x_>) \quad .$$

From here we get $q_L \approx f_L$ and $q_R \approx f_R$ where the omitted terms are of third order.

The direct transmission amplitude is

$$t_d \approx t_0 - \int f_L(x) f_R(x) dx \quad .$$

The direct transmission probability becomes

$$T_d \approx |t_0|^2 \left(1 - \int \frac{f_L(x) f_R(x)}{t_0} dx - \int \frac{f_L^*(x) f_R^*(x)}{t_0^*} dx\right) \quad .$$

Note that

$$M(x) = 2\,\mathrm{Re}\,\frac{q_R(x) q_L(x)}{t_d} \approx 2\,\mathrm{Re}\,\frac{f_R(x) f_L(x)}{t_0} \quad ,$$

which is of second order, as a result we can express T_d as

$$T_d \approx |t_0|^2 \left(1 - \int M(x) dx\right) \quad .$$

The transmission probability densities to the additional lines are

$$T_L(x) \approx |f_L(x)|^2 \quad , \qquad T_R(x) \approx |f_R(x)|^2 \quad ,$$

which are of second order. Therefore, the P matrix-function

$$P(x;y) = M(x)\delta(x-y) - \frac{2}{T_d} T_R(x_<) T_L(x_>) \quad ,$$

has at least a second order term as the first term and a fourth order term in the last term. For this reason, we might need to calculate $M(x)$ to fourth order as well. Let us consider the problem in the following way. Write the matrix as $P = P_1 + P_2$ where $P_1 = M(x)\delta(x-y)$ and P_2 is the remaining term. Inverse of P is

$$P^{-1} = P_1^{-1} - P_1^{-1} P_2 P_1^{-1} + P_1^{-1} P_2 P_1^{-1} P_2 P_1^{-1} - \cdots$$

Since $P_1^{-1} = M(x)^{-1}\delta(x-y)$, we have

$$\int\int T_R(x) P^{-1}(x;y) T_L(y) dx dy = \int \frac{T_R(x) T_L(x)}{M(x)} dx - \int\int \frac{T_R(x) P_2(x;y) T_L(y)}{M(x) M(y)} dx dy + \cdots \quad ,$$

where the first term is of second order and the second one is of fourth order. We keep the first term only. For this reason, we don't need to calculate the higher order terms in $M(x)$. The result for the dimensionless conductance is

$$g = |t_0|^2 \left(1 - \int M(x) dx\right) + 2 \int \frac{T_R(x) T_L(x)}{M(x)} dx \quad .$$

2.9 Summary

Here we summarize the steps of a numerical computation.

- A potential $V(x)$ has to be chosen and the solutions $\varphi_{L,R}$ of the Schrödinger equation at a selected energy E have to be obtained. We will use $\tilde{\varphi}_{L,R} = \sqrt{v_L}\varphi_{L,R}$ which are dimensionless. Through the solutions, we will also obtain the scattering matrix of the "bare" main line, the amplitudes r_0, r'_0 and t_0; but we will need only the transmission amplitude t_0.

- A decoherence interval (from x_L^D to x_R^D) has to be chosen and a function $\tilde{\gamma}(x)$ has to be defined on this interval. $\tilde{\gamma}(x)$ has the dimensions of Length$^{-1/2}$. It is related to $g(x)$ through the relation $\tilde{\gamma}(x) = g(x)/\hbar\sqrt{v(x)v_L}$. We will ignore the energy dependence of $\tilde{\gamma}$ and for all energies, E, use the same function.

- For the calculation, we will divide the interval $[x_L^D, x_R^D]$ into N subintervals each with length Δx_j and positioned at x_j. We will choose N to be large enough so that each subinterval is smaller than the wavelength of solutions (or smallest length scales associated with the wavefunctions $\tilde{\varphi}_{L,R}$).

- We are going to define $N \times 1$ column matrices f_{Lj} and f_{Rj} by

$$f_{Lj} = \tilde{\gamma}(x_j)\tilde{\varphi}_L(x_j)\sqrt{\Delta x_j} \quad , \qquad f_{Rj} = \tilde{\gamma}(x_j)\tilde{\varphi}_R(x_j)\sqrt{\Delta x_j} \quad ,$$

- We will construct the Γ matrix by

$$\Gamma_{j\ell} = \delta_{j\ell} + \frac{1}{t_0} f_{Rj_<} f_{Lj_>} \quad .$$

- We will obtain $N \times 1$ column matrices q_{Lj} and q_{Rj} by $q_L = \Gamma^{-1} f_L$ and $q_R = \Gamma^{-1} f_R$.

- The direct transmission amplitude will be calculated by using $t_d = t_0 - q_R^T f_L$ and the associated probability by $T_d = |t_d|^2$.

- The transmission probabilities from the left and right leads to the additional lines will be obtained by $T_{Lj} = |q_{Lj}|^2$ and $T_{Rj} = |q_{Rj}|^2$. Also, we will find m_j by

$$m_j = 2\,\mathrm{Re}\,\frac{q_{Rj}q_{Lj}}{t_d} \quad .$$

- We will define a matrix P by

$$P_{j\ell} = m_j \delta_{j\ell} - \frac{2}{T_d} T_{Rj_<} T_{Lj_>} \quad .$$

- Finally, the dimensionless conductance will be calculated by

$$g = T_d + 2T_R^T P^{-1} T_L \quad . \tag{2.22}$$

CHAPTER 3

RESULTS AND CONCLUSIONS

In this work we apply our model of continuum decoherence for the free particle, the single rectangular barrier, and the double barrier case in a one dimensional wire at mesoscopic scales. Incident electrons are described by plane waves. By appropriately defining length and energy scales, the Schrödinger equation can be written as

$$-\frac{d^2\psi(x)}{dx^2} + V(x)\psi(x) = E\psi(x) \quad .$$

We are going to work with this equation in this chapter. We consider potentials with $V(x \to -\infty) = V(x \to +\infty)$ so that $k_L = k_R$ and $v_L = v_R$. In this case $\frac{1}{\sqrt{v_L}}$ for φ_L and φ_R can be absorbed into γ, i.e.,

$$\tilde{\varphi}_L = \sqrt{v_L}\varphi_L \quad = \quad \begin{cases} \left(e^{ikx} + r_0 e^{-ikx}\right) & \text{for } x \to -\infty \\ \left(t_0 e^{ikx}\right) & \text{for } x \to +\infty \end{cases}$$

$$\tilde{\varphi}_R = \sqrt{v_L}\varphi_R \quad = \quad \begin{cases} \left(t_0 e^{-ikx}\right) & \text{for } x \to -\infty \\ \left(e^{-ikx} + r_0' e^{ikx}\right) & \text{for } x \to +\infty \end{cases}$$

$\tilde{\gamma}_j = \frac{\gamma_j}{\sqrt{v_L}}$ so $f_{R,j} = \tilde{\gamma}_j \tilde{\varphi}_R(x_j)$. In this case $\tilde{\varphi}_{L,R}$ and $\tilde{\gamma}$ are dimensionless. Calculating $f_{R,j}$ and $f_{L,j}$ we will get

$$\Gamma_{j\ell} = \delta_{j\ell} + \frac{1}{t_0} f_{Rj_<} f_{Lj_>} \quad .$$

Then we will calculate

$$q_L = \Gamma^{-1} f_L$$

and

$$q_R = \Gamma^{-1} f_R.$$

Next step is calculating

$$T_{Lj} = |q_{Lj}|^2$$

and

$$T_{Rj} = |q_{Rj}|^2$$

and from here

$$t_d = t_0 - q_R^T f_L.$$

Then we will find

$$T_d = |t_d|^2$$

and

$$m_j = 2\,\mathrm{Re}\,\frac{q_{Rj} q_{Lj}}{t_d}$$

to construct the matrix P

$$P_{j\ell} = m_j \delta_{j\ell} - \frac{2}{T_d} T_{Rj_<} T_{Lj_>} \quad .$$

Finally we will get conductance as

$$g = T_d + 2T_R^T P^{-1} T_L \quad .$$

All the details about these calculations are shown in Chapter 2.

3.1 Free particle case

First, we apply the decoherence model to free particles where there is no scatterer. A decoherence interval with length L is chosen and $\tilde{\gamma}(x)$ is defined on this interval for the chosen N points. By taking N large enough we guarantee that each subinterval is smaller than the wavelength of the solutions. $\tilde{\gamma}(x)$ is related to $g(x)$, which shows the coupling strength to the additional lines, through the relation $\tilde{\gamma}(x) = g(x)/\hbar\sqrt{v(x)v_L}$. Decoherence interval from x_L^D to x_R^D shown in Fig. 3.1. For simplicity, we take $\tilde{\gamma}(x)$ to have the constant value D/L over the decoherence interval of length L. Here D is

$$D = \int \tilde{\gamma} dx.$$

In Fig. 3.2 conductance versus $k_F L$ graph for D=1 is shown. Because of wave nature we see oscillations at the right part of the graph. In Fig. 3.3 conductance

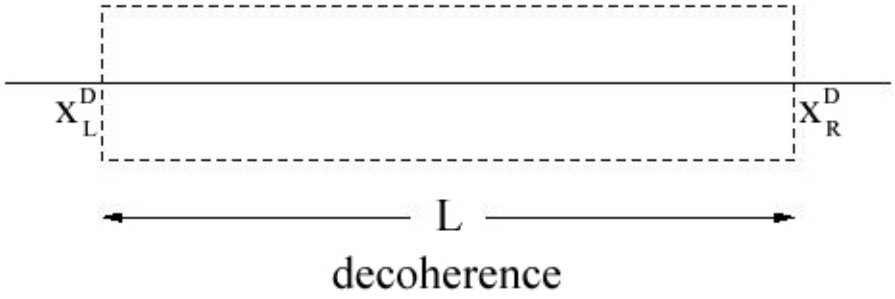

Figure 3.1: V=0 everywhere. A decoherence interval is chosen and $\tilde{\gamma}(x)$ is defined on this interval.

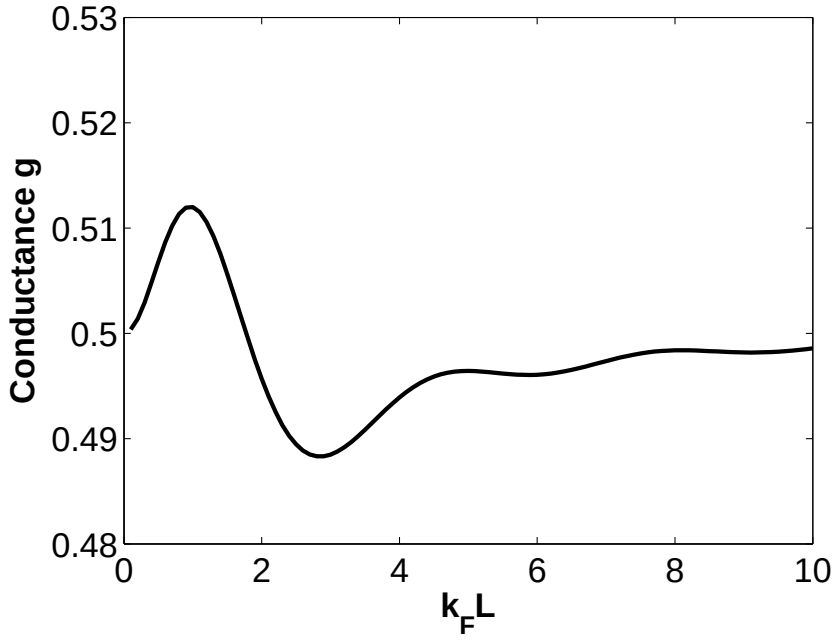

Figure 3.2: Conductance versus k_FL for D=1.

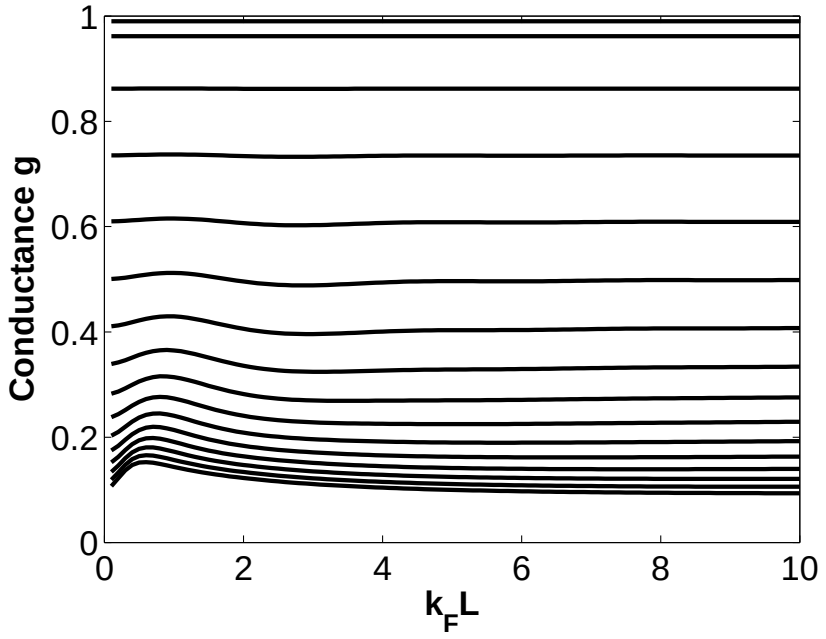

Figure 3.3: Conductance versus k_FL for different D values. D gets values 0.1, 0.2, 0.4, 0.6, 0.8, 1, 1.2, 1.4, 1.6, 1.8, 2, 2.2, 2.4, 2.6, 2.8, 3 from top to bottom.

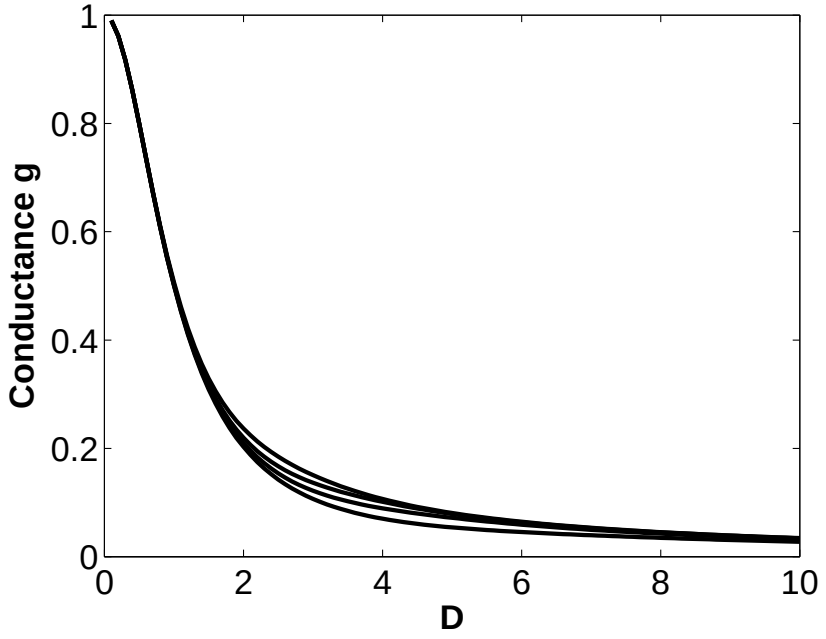

Figure 3.4: Conductance versus D for k_FL smaller than 1. k_FL gets values 0.1, 0.2, 0.3, 0.5 from bottom to top.

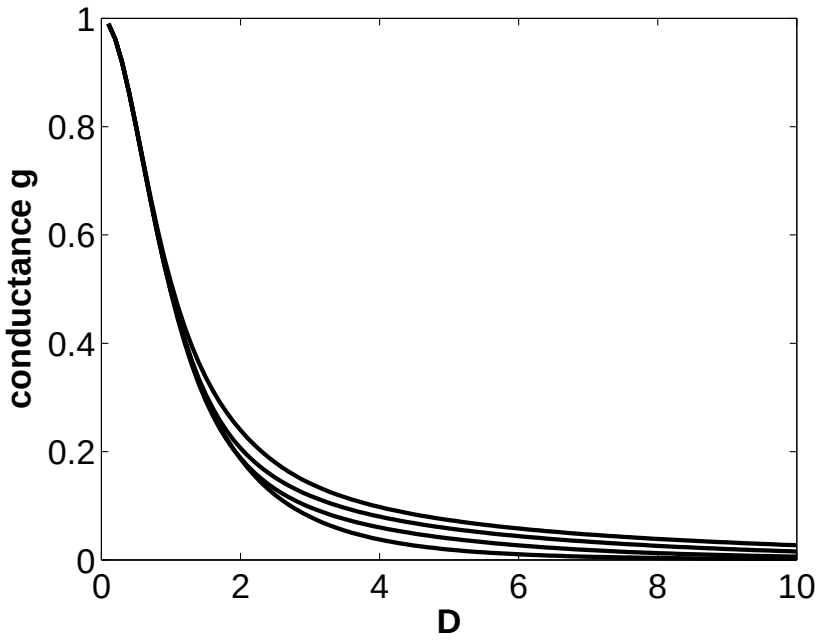

Figure 3.5: Conductance versus D for k_FL bigger than 1. k_FL gets values 1, 2, 4, 10 from top to bottom.

versus $k_F L$ graph for different D values is shown. It can be seen that although the conductance depends on $k_F L$, this dependence is very weak. For that reason, the value of D determines the value of the conductance in a rough way.

In Fig. 3.4 conductance versus D graph for different $k_F L$ values are shown. In this graph $k_F L$ values are smaller than 0.5 and the conductance is increasing as $k_F L$ is approaches to approximately 0.5. But the situation is reversed when $k_F L$ is bigger than 0.5. We see in Fig. 3.5 that the conductance is decreasing as $k_F L$ is increasing in that case.

3.2 Single rectangular barrier case

Next, we investigate the case where the scatterer is a single rectangular barrier. The potential felt by the electrons is shown in Fig. 3.6. Electron waves tunnel through the single rectangular barrier. Wave amplitudes are calculated by just matching the wave functions and their derivatives at the barrier's boundaries. Once we get the wavefunctions φ_L and φ_R, we again apply the same procedure to obtain conductance g.

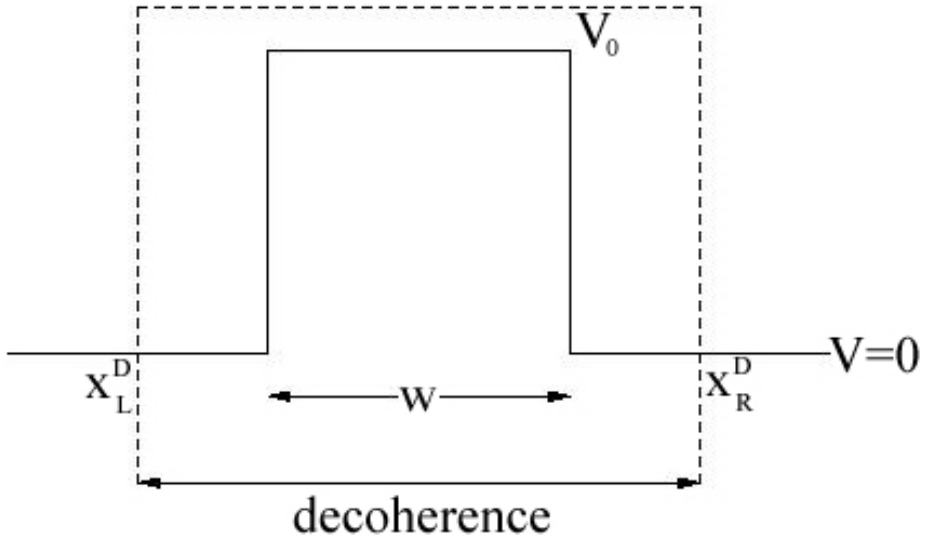

Figure 3.6: Single rectangular barrier case.

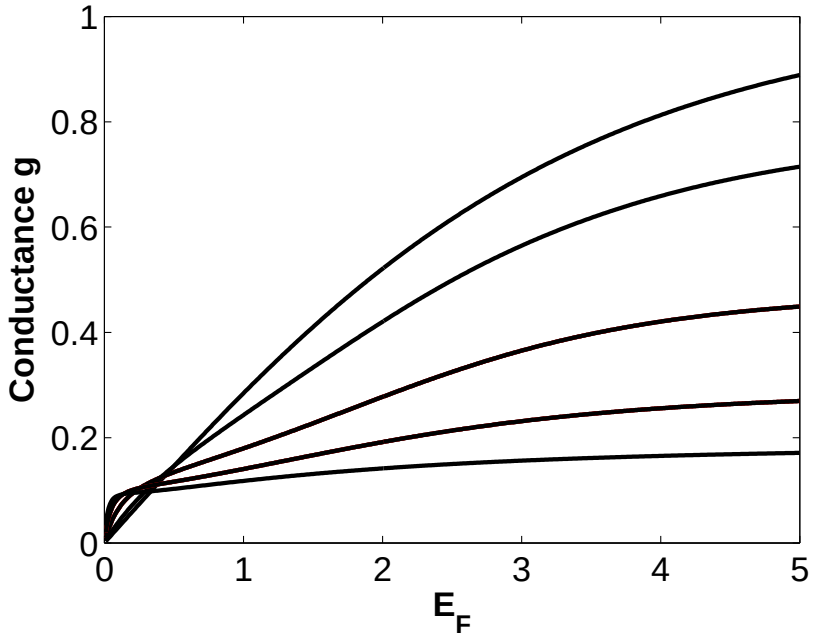

Figure 3.7: Conductance vs E_F graph for different D values. D gets values 0, 1, 1.5, 2, 2.5 from top right to bottom right.

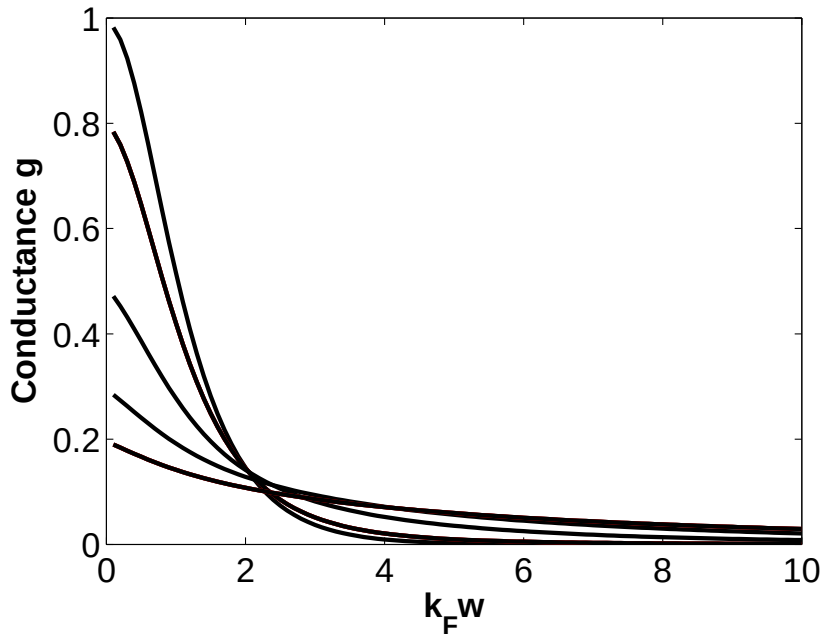

Figure 3.8: Conductance vs $k_F w$ graph for different D values and for some fixed $E(< V_0)$. D gets values 0.1, 0.5, 1, 1.5, 2 from top left to bottom left.

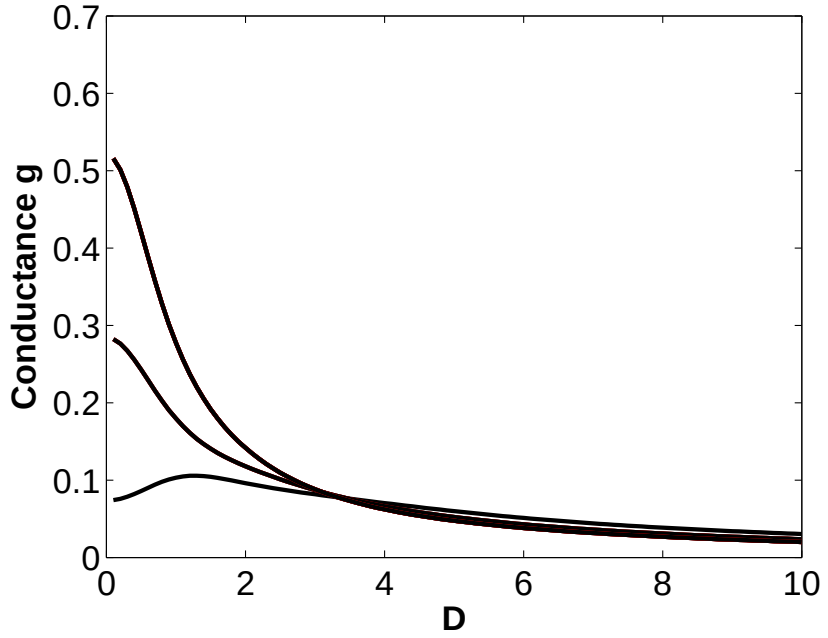

Figure 3.9: Conductance vs D graph for $E = 0.25, 1, 2(< V_0 = 2.5)$ from top left to bottom left.

In Fig. 3.7 conductance versus E_F graph is depicted for different D values. Fig. 3.7 shows that after the tunnelling region and including some parts of the tunnelling region, as decoherence increasing the conductance g decreases. But in low energy part of the tunnelling region as decoherence increasing the conductance g also increases. As we see decoherence also effects the tunnelling transmission.

Fig. 3.8 shows how the width of the barrier effects the conductance for some fixed $E(< V_0)$. In Fig. 3.8 conductance versus $k_F w$ graph is shown for different D values and $E = 2(< V_0 = 2.5)$. We see that as decoherence is increasing the conductance g is decreasing and also the conductance g is getting smaller as the width of the barrier is getting bigger. Finally, Fig. 3.9 shows conductance versus D graph for $E = 0.25, 1, 2(< V_0 = 2.5)$.

3.3 Double barrier case

Finally, we investigate a scatterer formed by two rectangular barriers. Electron waves tunnel through the left and right barriers via a well-like region with length L. The potential felt by the electrons is depicted in Fig. 3.10. In the well, the electron wave experiences multiple reflections due to the barriers and then the wave tunnels out the right barrier. Transfer matrix method is used to calculate the reflection and transmission coefficients. The barriers' transfer matrices are obtained by matching the wave functions and their derivatives at the boundaries. From here we get the transmission and reflection amplitudes. Once we get the transmission probability we apply our procedure mentioned in Chapter 2 to get the conductance g.

Fig. 3.11 shows conductance versus E_F graph for different D values for the double barrier case. As can be seen in the figure, the conductance decreases with the increase in decoherence. D=0 case is shown at the top. The peaks seen in the tunnelling region, where the energies are smaller than $V_0 = 2.5$, are due to resonant transmission. In this region we see that decoherence makes the constructive interference of electron waves disappear. As a result, we see that the conductance, i.e., the electron transmission, is suppressed by dephasing. Similarly, after that region we see that conductance is suppressed by dephasing.

Fig. 3.12 shows conductance versus D graph for $E_F = E_1 = 0.96$ and for $E_F = E_2 = 1.41$ which is the second maximum and second minimum at Conductance vs

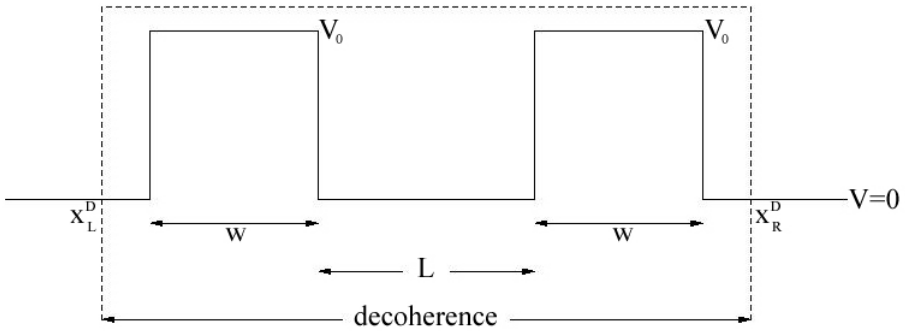

Figure 3.10: Double barrier case.

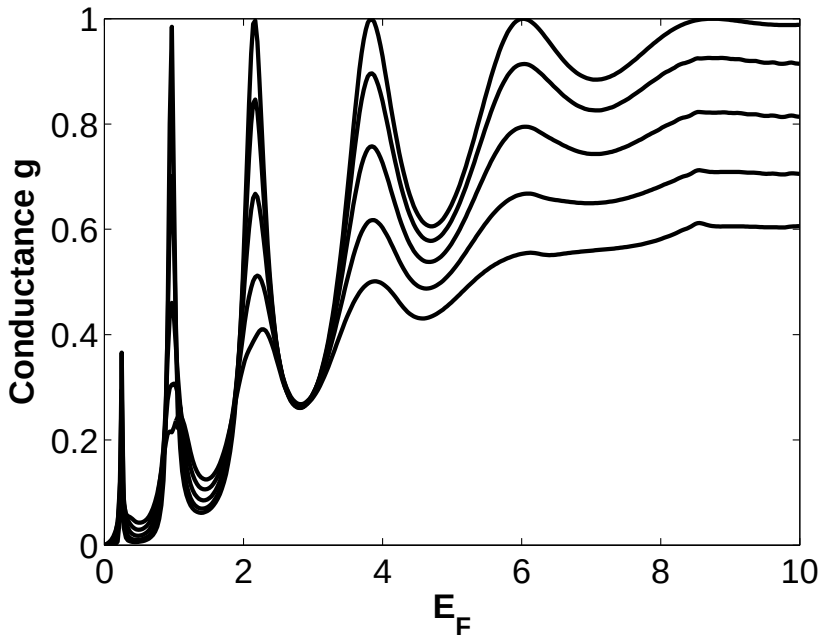

Figure 3.11: Conductance vs E_F graph for different D values. D gets values 0, 0.3, 0.5, 0.7, 0.9 from top right to bottom right.

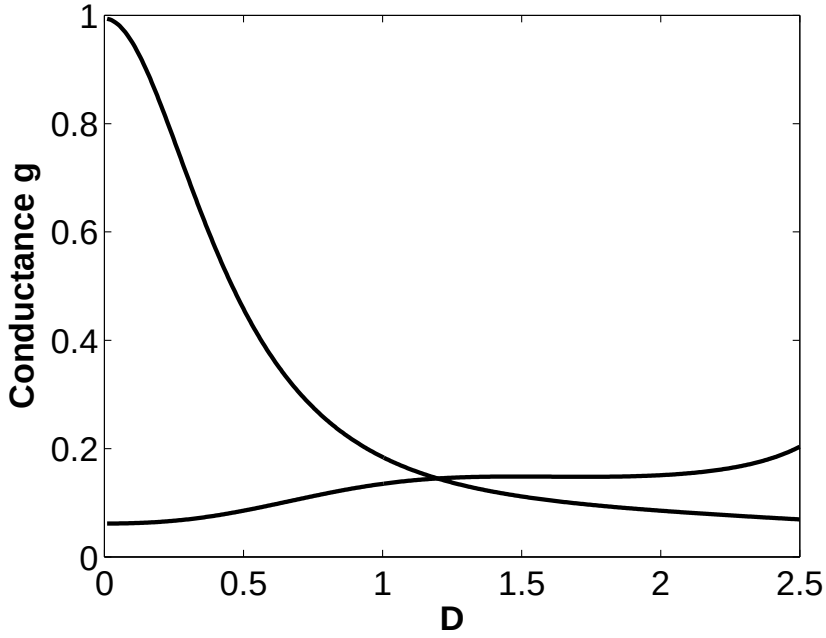

Figure 3.12: Conductance vs D graph for $E_F = E_1 = 0.96$ which is the second maximum at Conductance vs E_F graph for different D values(Fig. 3.11) and for $E_F = E_2 = 1.41$ which is the second minimum in the same Fig. 3.11.

E_F graph for different D values (Fig. 3.11).

3.4 Discussions and Conclusions

In this work we have numerically investigated our continuum model for decoherence in 1D transport through a mesoscopic wire. The dephasing effects in 1D transport had been investigated by extending Büttiker dephasing model, which is a conceptually simple model to simulate the dephasing effect in 1D transport through a mesoscopic system by coupling an electron reservoir to the conductor. In our model decoherence proceeds at every location. To achieve that we coupled 2N electron reservoirs to the conductor by 2N channels and we took $N \longrightarrow \infty$ limit to obtain the continuum case. In the reservoirs, inelastic events and phase randomization take place. Electrons can go to equilibrium in those channels but will eventually return back into the conductor. However, they will have lost phase coherence with the electrons in the conductor.

Decoherence mainly prevents wave interference. Depending on whether the in-

terference increase or decrease the transmission probability, decoherence may decrease or increase the conductance. So, if constructive interference is present in the forward direction, decoherence will prevent that and decrease the conductance. Otherwise, if destructive interference is effective in the forward direction, then decoherence increases the conductance. But as a rough guide we can give the following rule: When the transmission probability is roughly below 0.1, decoherence increases the conductance. Otherwise, if the transmission probability is above 0.1, then decoherence decreases the conductance.

Our model is more consistent with the prevalent notions of decoherence since the placement of the single scatterer in Büttiker's model effects the electron transmission. In Büttiker's model, voltage probe is placed at a single chosen point. This corresponds to a small decoherence interval, for example in the middle of a double barrier as shown in Fig. 3.13.[17] Consider the conductance versus energy graph of this sytem for D=0, which is shown in Fig. 3.14. Let us consider the two possible Fermi energies, $E_F = 0.2501$ and $E_F = 0.9700$ which corresponds to the first two resonant transmission maxima. Conductance versus D graphs for these energies are plotted in Fig. 3.15. It can be seen that for $E_F = 0.2501$, the decoherence is very effective and the conductance decreases quite rapidly with increasing D. On the other hand, for $E_F = 0.9700$, although the conductance depends on D, it decreases much more slowly.

The main reason for such a different behavior is shown in Fig. 3.16 and Fig. 3.17 where the left incident wavefunctions are plotted. For $E_F = 0.2501$, the wavefunction shown in Fig. 3.16 has a peak at the location of the voltage probe. Therefore, the electrons at the Fermi level couple strongly to the probe. On the other hand, for $E_F = 0.9700$, the wavefunction shown in Fig. 3.17 has almost a node at the middle. Therefore, it couples weakly to the probe. As a result, decoherence appears to be very effective for the first and ineffective for the second.

In general, the detailed behavior of the wavefunctions at the point the voltage probe is placed is very important. And, usually it is possible to obtain conductance features that depends on the placement of the probe, which might appear contrary to intuition. If decoherence proceeds in a wide region, such artificial features will disappear. For example, in our model, the conductance versus D graph for $E_F =$

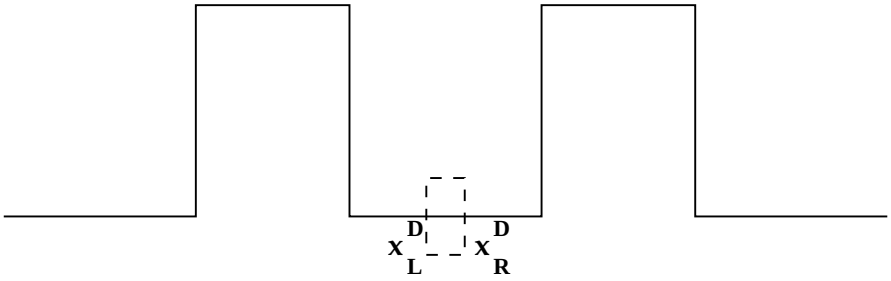

Figure 3.13: Büttiker's model for decoherence.

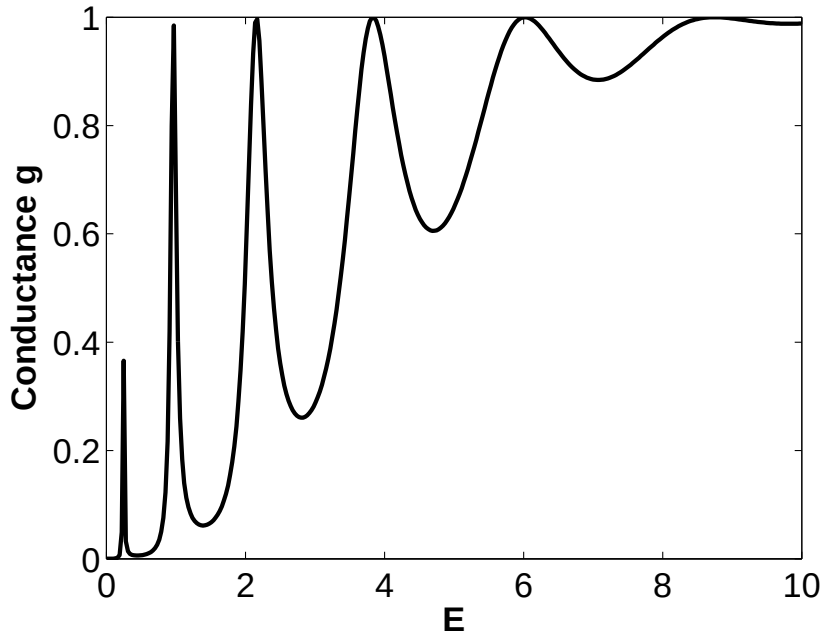

Figure 3.14: Conductance vs E_F graph for D=0 in Büttiker's model.

0.9700 is shown in Fig. 3.12 where it is seen that, g indeed decreases quite rapidly with increasing D.

In summary, we have proposed a model to address the significant dephasing effects in 1D transport. And we have observed that dephasing can dramatically change the conductance of a conductor since it effects the transmission probability of the electron waves.

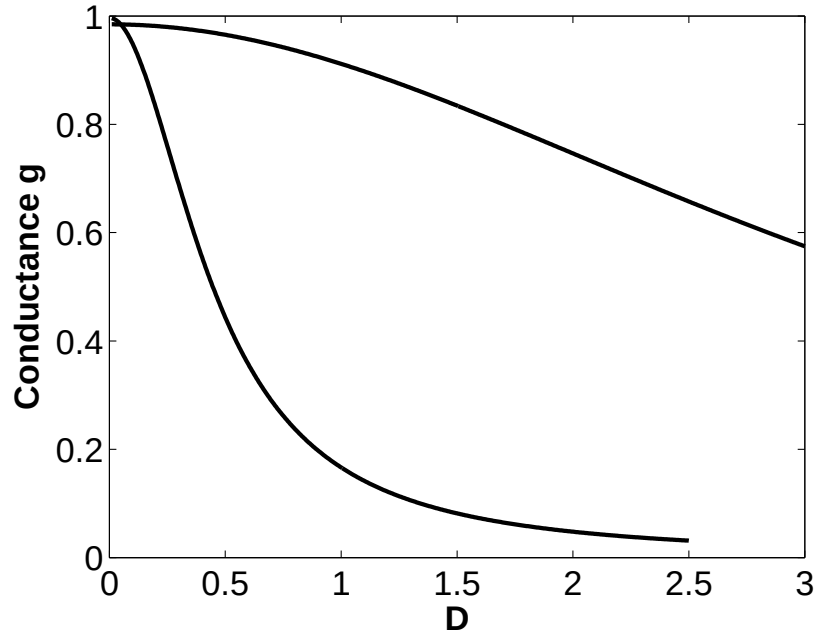

Figure 3.15: Conductance vs D graph for E=0.25 and 0.97 the first and the second maximum in Fig. 3.14.

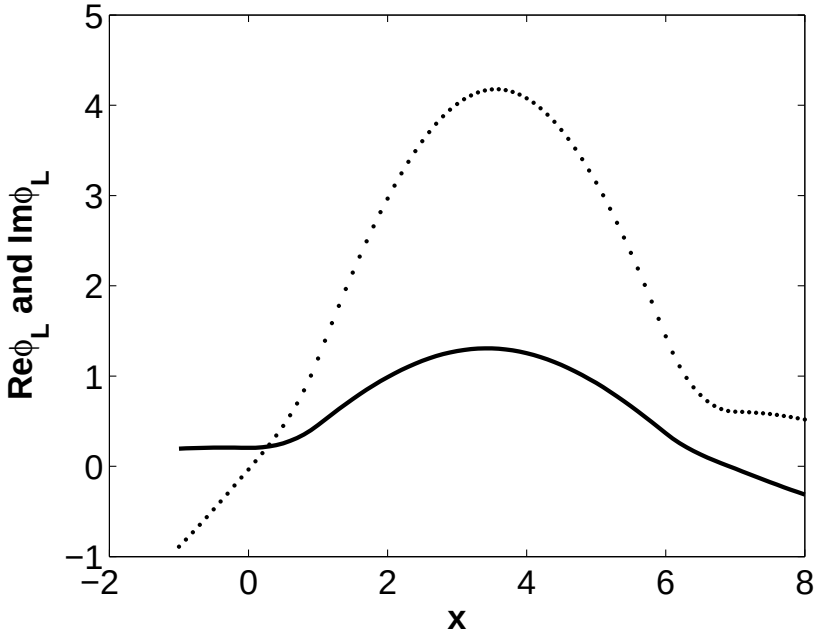

Figure 3.16: Position vs real and imaginary parts of the wavefunction for E=0.25 first maximum in Fig. 3.14. Solid line, real part of the wavefunction; dotted line, imaginary part of the wavefunction.

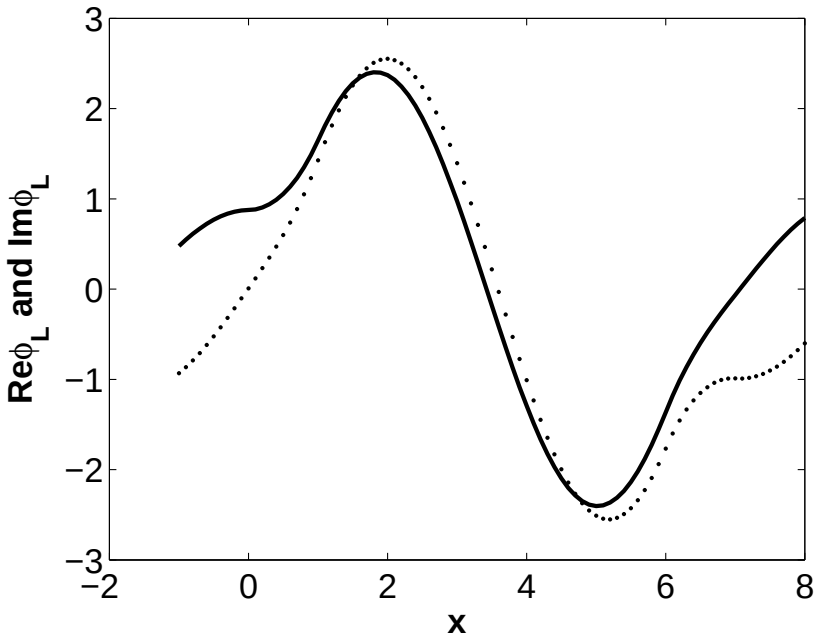

Figure 3.17: Position vs real and imaginary parts of the wavefunction for E=0.97 second maximum in Fig. 3.14. Solid line, real part of the wavefunction; dotted line, imaginary part of the wavefunction.

.

REFERENCES

[1] H. A. D. A. G. D. T.J. Thornton, M. Pepper *Phys. Rev. Lett.*, vol. 56, p. 1198, 1986.

[2] L. K. H. v. H. C. B. J. M. C. F. B, J. Wees and J. Harris *Phys. Rev. B*, vol. 38, p. 3625, 1988.

[3] R. N. M. P. H. A. J. F. D. H. D. P. D. R. D.A. Wharam, T.J. Thornton and G. Jones *Solid State Phys.*, vol. 21, p. L209, 1988.

[4] R. L. M. Büttiker, Y. Imry and S. Pinhas *Phys. Rev. B*, vol. 31, p. 6207, 1985.

[5] M. Namiki, S. Pascazio, and H. Nakazato, *Decoherence and Quantum Measurements*. World Scientific Publishing Co. Pte. Ltd., 1997.

[6] R. Feynman, R. B. Leighton, and M. L. Sands, *The Feynman Lectures on Physics III Chapter 1*. Addison-Wesley Publishing, 1965.

[7] F. Marquardt, "An introduction to the basics of dephasing," tech. rep., University of Basel, 2001.

[8] C. Benjamin, "Electron transport and quantum interference at the mesosocopic scale," tech. rep., Università degli Studi di Salerno, 2004.

[9] Y. Imry, *Introduction to Mesoscopic Physics*. Oxford University Press. New York, 1997.

[10] Y. Imry, "Quantum dephasing in mesoscopic systems," in *Proceedings of the 6th International Symposium on Foundations of Quantum Mechanics in the Light of New Technology*, August 1998.

[11] D. Landauer *IBM J. Res. Dev.*, vol. 1, p. 223, 1957.

[12] R. Landauer *Philos Mag.*, vol. 21, p. 863, 1970.

[13] S. Datta, *Electronic Transport in Mesoscopic Systems*. Cambridge University Press, 1995.

[14] A. Çipiloğlu, *Thermoelectric Effects in Mesoscopic Physics*. PhD thesis, Middle East Technical University, 2004.

[15] C. Benjamin and A. M. Jayannavar *Condensed Matter*, vol. 1, p. 0209438, 2002.

[16] C. Benjamin and A. M. Jayannavar *Condensed Matter*, vol. 2, p. 0203010, 2003.

[17] M. Büttiker, "Role of quantum coherence in series resistors," *Phys. Rev. B*, vol. 33, no. 5, pp. 3020–3026, 1986.

[18] M. Büttiker *IBM J. Res. Develop.*, vol. 32, pp. 63–75, 1988.

[19] X.-Q. Li and Y. Yan *Phys. Rev. B*, vol. 65, p. 155326, 2002.

APPENDIX A

INVERSE OF MATRICES OF A SPECIAL TYPE

Consider an $N \times N$ matrix of the form

$$F_{nm} = \delta_{nm} + \lambda s_{n_<} b_{n_>} \quad ,$$

where s_n and b_n are arrays of size N. We will consider s and b as N dimensional column vectors. The matrix F looks like,

$$F = \begin{bmatrix} 1+\lambda s_1 b_1 & \lambda s_1 b_2 & \lambda s_1 b_3 & \cdots \\ \lambda s_1 b_2 & 1+\lambda s_2 b_2 & \lambda s_2 b_3 & \cdots \\ \lambda s_1 b_3 & \lambda s_2 b_3 & 1+\lambda s_3 b_3 & \cdots \\ \vdots & \vdots & \vdots & \ddots \end{bmatrix}$$

Note that F is symmetric: $F^T = F$. We will show below that the inverse of F, if it exists, is of the same form.

First, consider the matrix $F' = F - \lambda s b^T$. Its matrix elements and its matrix are

$$F'_{nm} = \begin{cases} \delta_{nm} & \text{if } n \leq m \quad , \\ \lambda(s_m b_n - s_n b_m) & \text{if } n > m \quad , \end{cases}$$

$$F' = \begin{bmatrix} 1 & 0 & 0 & \cdots \\ \lambda(s_1 b_2 - s_2 b_1) & 1 & 0 & \cdots \\ \lambda(s_1 b_3 - s_3 b_1) & \lambda(s_2 b_3 - s_3 b_2) & 1 & \cdots \\ \vdots & \vdots & \vdots & \ddots \end{bmatrix}$$

In other words, F' is lower triangular and all of its diagonal elements is 1. In that case the inverse $(F')^{-1}$ exists, is lower triangular and all of its diagonal elements are

one. If F is invertible, $(F')^{-1}$ can be written as

$$\begin{aligned}(F')^{-1} &= (F-\lambda s b^T)^{-1} = \left(F(I-\lambda F^{-1} s b^T)\right)^{-1} = (I-\lambda F^{-1} s b^T)^{-1} F^{-1} \\ &= F^{-1} + \lambda F^{-1} s b^T F^{-1} + \lambda^2 F^{-1} s b^T F^{-1} s b^T F^{-1} + \cdots \\ &= F^{-1} + \lambda(1+\lambda\alpha+\lambda^2\alpha^2+\cdots) F^{-1} s b^T F^{-1} \\ &= F^{-1} + \frac{\lambda}{1-\lambda\alpha} F^{-1} s b^T F^{-1} \\ &= F^{-1} - \lambda' s' b'^T\end{aligned}$$

where

$$\alpha = b^T F^{-1} s \quad , \quad s' = F^{-1} s \quad , \quad b' = F^{-1} b \quad , \quad \lambda' = -\lambda/(1-\lambda\alpha) \quad . \tag{A.1}$$

Finally we use the fact that $((F')^{-1})_{nm} = \delta_{nm}$ for $n \leq m$ to find $(F^{-1})_{nm} = \delta_{nm} + \lambda' s'_n b'_m$. Using the symmetry of F we get

$$(F^{-1})_{nm} = \delta_{nm} + \lambda' s'_{n_<} b'_{n_>} \quad . \tag{A.2}$$

Note that if the dimension N is large, the lower triangular matrix F' can be used for faster numerical calculations of s' and b' by

$$\begin{aligned}s' &= (1-\lambda\alpha)(F')^{-1} s \quad , \\ b'^T &= (1-\lambda\alpha) b^T (F')^{-1} \quad , \\ (1-\lambda\alpha) &= \left(1+\lambda b^T (F')^{-1} s\right)^{-1} \quad .\end{aligned}$$

Second, if another diagonal matrix is contained in F instead of identity, the same results can be obtained. For

$$F_{nm} = f_n \delta_{nm} + \lambda s_{n_<} b_{n_>} \quad ,$$

the inverse is given by

$$F^{-1}_{nm} = \frac{1}{f_n}\delta_{nm} + \lambda' s'_{n_<} b'_{n_>} \quad ,$$

where λ', s', b' and α can be calculated by using the expressions in Eq. (A.1). They can also be calculated by using the triangular matrix as shown above.